Development and implementation of an operational surface ozone objective analysis with CHRONOS model and AIRNOW observations

Alain Robichaud
Richard Ménard

Novembre 2003

INDEX

ABSTRACT

Objective analysis (OA) is an essential first step in building up an assimilation system. Producing maps of objective analysis on a regular basis is motivated by many factors such as: 1) to initialize models, 2) to provide users with a spatially complete and accurate analysis (as compared to model output or observations alone) and 3) to bring deep insights into possible model erroneous behavior or bugs.

In this study, CHRONOS model (v2.3.6) for surface ozone is used since CHRONOS model error statistics could be produced in an easy way over most of North America. On the other hand, EPA-AIRNOW ozone real-time data base is also available for surface ozone observations for a large part of North America. Data from over 1400 stations are collected on a hourly basis from this data base making the production of Objective analysis and data assimilation an attractive issue for surface ozone.

The problem of Objective analysis is the same as Optimal Interpolation and is posed here as a problem of statistical optimization. With no data selection on observing stations, it becomes equivalent to a 2D-VAR (two-dimensional variational analysis). It was found that a FOAR representation (First Order Autoregressive Model) is more suitable to estimate CHRONOS model error statistics for surface ozone than SOAR (Second Order Autoregressive model) or TOAR (Third Order Autoregressive model) fittings usually adopted in meteorology for Objective analysis or data assimilation. Finally, it was also demonstrated that not removing the bias of innovation at each station gives better results (higher score for the correlation between OA against observations) as compared to the case when the bias of innovation is removed.

Verification of Objective analysis outputs versus observations in both R&D (off-line) and operational mode (on-line) have demonstrated good results so far for surface ozone and implementation on an experimental basis started on July 4th 2003 at CMC. The sub-grid scale representativeness issue remains to be addressed in the future especially for the case of some reporting stations which display strong local behavior.

SOMMAIRE

L'analyse objective (AO) est une première partie essentielle dans le processus d'assimilation. La production de cartes AO sur une base routinière est motivée par plusieurs facteurs tels que : 1) initialisation des modèles, 2) fournir aux utilisateurs une analyse complète et précise (comparé aux sorties de modèles ou aux observations prises séparément) et 3) permet d'examiner en profondeur le comportement du modèle et de détecter des erreurs.

Dans la présente étude, le modèle CHRONOS (v2.3.6) pour la prédiction de l'ozone de surface est utilisé. Les erreurs de modèle peuvent être facilement produites sur tout l'Amérique du Nord. D'autre part, les données de surface d'ozone en temps réel sont aussi disponibles pour une grande partie de l'Amérique du Nord. On collecte les données de plus de 1400 stations sur une base horaire. Ainsi, la production d'une carte d'analyse objective ou de l'assimilation des données devient une option attractive pour l'ozone de surface.

Le problème de l'analyse objective est le même que celui de l'interpolation optimale et est posé ici en termes d'optimisation statistique. Lorsqu'il n'y a aucune sélection des stations d'observations, le problème devient équivalent au 2D-VAR (analyse variationelle en deux dimensions). On a trouvé qu'une représentation de type FOAR (modèle autorégressif du premier ordre) constitue un meilleur estimé pour les statistiques d'erreur du modèle CHRONOS que des représentations de type SOAR (modèle autorégressif du second ordre) ou TOAR (modèle autorégressif du troisième ordre) usuellement adoptés en météorologie dans le contexte de l'analyse objective et de l'assimilation. Finalement, on démontre que si le biais des innovations n'est pas enlevé, de meilleurs résultats sont obtenus (coefficient de corrélation plus élevé entre AO et les observations) par rapport au cas où le biais est enlevé.

La vérification de l'AO avec les observations en modes R&D (off-line) et opérationnel (on-line) ont démontré de bons résultats. L'implémentation sur une base expérimentale a débuté le 4 juillet 2003 au CMC. La représentativité sous-maille de certaines stations de mesure montrant des effets locaux importants est un sujet d'intérêt qui sera examiné dans le futur dans le contexte de l'assimilation.

1) INTRODUCTION

Objective analysis is an essential first step in building up an assimilation system. Producing maps of objective analysis (OA) on a regular basis is motivated by many factors such as:

1) to initialize numerical models at regular time interval (usually every 6 or 12 hours) with appropriate fields having overall bias and error variance which are minimum,

2) to provide users with a more accurate picture of the true state of a given variable by using an appropriate optimal blend of model fields together with observations so that it produces the best possible analysis not only in the vicinity of observation points but everywhere in a given domain even where the observation network is sparse,

3) to trace back possible bugs that went undetected either with the numerical model or with the observation system (this is done by identifying regular or systematic patterns appearing on the analysis increment field).

Objective analysis is posed here as an optimization problem. The basic goal is to find an expression which will minimize the error variance of the combined field of model and observation. The classical theory of optimal interpolation (OI) has been applied here.

In meteorology, objective analysis have been used extensively over the past 20 years or so to initialize models (Daley, 1991; Mitchell et al., 1996). The first Objective analysis was implemented here at CMC in the 70's for the 500 mbs wind field obtained from radiosondes (Rutherford, 1972). Today, objective analysis is produced on a routinely basis of many meteorological fields at different levels (including the surface) in many countries in the world. Algorithms such as 3D-VAR or 4D-VAR (three or four dimensional variational analysis) are used on a routine basis to assimilate different types of data (satellite, radiosondes, buoys, ship or airplane reports, surface measurements, etc.).

In the field or air quality, data assimilation is now emerging at a rapid pace. However, at the surface, data assimilation of chemical species is still in its infancy. Very few attempts have been made so far and those were achieved with mitigated success. It has been found that it is rather difficult to obtain good error statistics for surface observations for regional or large-scale chemical transport models (see for example, Tilmes, 1999 for Germany). Many reasons could explain this fact: surface observations are too close to sources, topography destroys the model error covariance signal with distance, difficulty to share regional or global error statistics among countries or different parts of the same country (this is thought to be the case in US), etc.

In this study, CHRONOS model is used since model error statistics could be produced over most of North America. On the other hand, EPA-AIRNOW data base is available for surface ozone observation for a large part of US and many parts of Southern Canada. Moreover, the relatively flat topography found over Eastern North America and the importance of transport of ozone above the boundary layer makes surface ozone an

excellent candidate for objective analysis and data assimilation in North America and particularly for Canada[1].

2) THEORY

Basics of Optimal Interpolation

The problem of Objective analysis is the same as Optimal Interpolation and is posed here as a problem of statistical optimization.

The basic equation of objective analysis or optimal interpolation (OI) is

$$X_a = X_b + K(y^o - HX^b) \qquad (1)$$

where the different components of the equation are defined below:

X_a: objective analysis field matrix (dimension 350 X 250)
X_b: trial field (forecast from CHRONOS model) (dimension 350 X 250)
K : gain matrix (dimension 350 X 250 X NS)
y^o: observation vector (dimension NSX1).
H: interpolation operator for model at the station location (cubic semi-Lagrangian or linear).

Equation 1 simply states the fact that we want an analysis to depend linearly on observation departures from model. The dimension 350X250 corresponds to the current CHRONOS grid model (Version 2.3.6) and NS is the number of reporting stations utilized in the objective analysis (OA).

It can be shown that the formulation of the K matrix which minimizes the variance of analysis (var (X_a)) is given by (see, for example, Bouttier et Courtier, 2000);

$$K = (HP^f)^t \, (H(HP^f)^t + R)^{-1} \qquad (2)$$

with the symbols defined below:
P^f : model forecast error covariance matrix (NS X NS)
^{t} : transpose of a matrix
R : observation error covariance matrix (dimension is NS X NS; with R being a diagonal matrix).

In equation 2, a basic assumption is that observation error (R) and forecast error (P^f) are supposed to be not statistically correlated. The quantity, $y^o - HX^b$, is called the innovation and represents the value of observation minus interpolated model value at point of observation (dimension NS X 1). Note that observation error R refers to interpolation error and instrument error lumped together. The term $H(HP^f)^t$ in equation 2, represents the model forecast error covariance between observation locations k_1 and k_2, and is supposed of the form:

[1] This will be even more true if the existing network of stations in Canada would be expanded to cover a bigger area of Canada so more data is available in the assimilation system.

$$H(HP^f(k_1,k_2))^t = \sigma_f(k_1)\,\sigma_f(k_2)\exp\{ - |x(k_1)- x(k_2)|/L_c \} \quad (3)$$

where σ_f is the model forecast error evaluated at a given point, **x** is position vector for a given reporting station and L_c , a quantity so-called the correlation length. In this report, L_c is assumed to be constant over the domain for a given hour.

The only remaining quantity to be defined in equation (2) is $(HP^f)^t$. The following expression describes the latter quantity, that is;

$$(HP^f(i,j,k_1))^t = \sigma_f(i,j)\,\sigma_f(k_1)\exp\{ - |x(i,j)- x(k_1)|/L_c \} \quad (4).$$

In equation (4), $\sigma_f(i,j)$ is taken as a constant since it was not possible, in this study, to evaluate the model error at a grid point i,j (that is in the model space). Note, however, that in equation (3), since σ_f is evaluated in the observation space, a value is available for each observing station. The averaged domain value of σ_f in the observation space is then used as a mean for $\sigma_f(i,j)$ in equation (4) (i.e in model or grid space). There is no radius for data selection of observing stations for a particular grid point so that this generalized OI is equivalent to a variational analysis in two dimension (2D-VAR).

The main hypothesis of statistical interpolation are that observation and model errors are not biased and not statistically correlated between each other. The operator H must also be linear otherwise other methods must be used to find the matrix K which minimizes the error variance of X_a. Error statistics (innovation) does not necessarily obey a Gaussian distribution but if they do then X_a is also the maximum likelihood estimator of the true state (Bouttier et Courtier, 2000).

The matrix A given below (which is the right hand side of equation 2) has to be inverted only once for a given hour and is valid for each grid point, that is;

$$A^{-1} = (H(HP^f)^t + R)^{-1} = (HP^fH^t + R)^{-1} \quad (5).$$

One potential problem of (5) is when the matrix A becomes so big that it cannot be inverted. If this is the case, other methods (outside the scope of this study) must be used to get K in equation (1). Otherwise, the matrix A must be positive definite (all eigenvalues must be greater than zero) and symmetrical. Tests done in the context of this report show that A is always symmetrical and positive definite. The conditions of having eigenvalues of A being positive and non-zero has been successfully tested in cases where the number of stations NS is below 1500 for surface ozone in North America with CHRONOS V2.3.6.

Chi-square diagnostic

In the validation phase, the Chi-square diagnostic is used to verify the model error covariances in data assimilation systems (Ménard et al. 1999). In the observation space, it is defined as an inner-product of the form:

$$X^2/NS = \nu A^{-1} \nu^t \qquad (6)$$

where ν and ν^t are respectively the innovation vector and its transpose and A^{-1} is the inverse of the innovation covariance matrix.

As an average, X^2/NS must be close to a value around 1 where NS is the number of stations used in the OA system. Values outside the range 0.5 to 2.0 (in the case of unbiased innovation) usually indicates the presence of problems or bugs in the system since the real-time covariance of innovation then no longer match (at least within a factor 2) the prescribed innovation covariance given in equation (5).

3) OBSERVATIONS AND TOOLS USED

Observations collected from different surface ozone network across North America is gathered in EPA-AIRNOW data base on a real-time basis (ftp.epa.gov/airnow/products). Data from over 1400 stations is collected on a hourly basis from this data base. Figure 1 shows the distribution of stations monitoring surface ozone that are potentially available for objective analysis (July 2003).

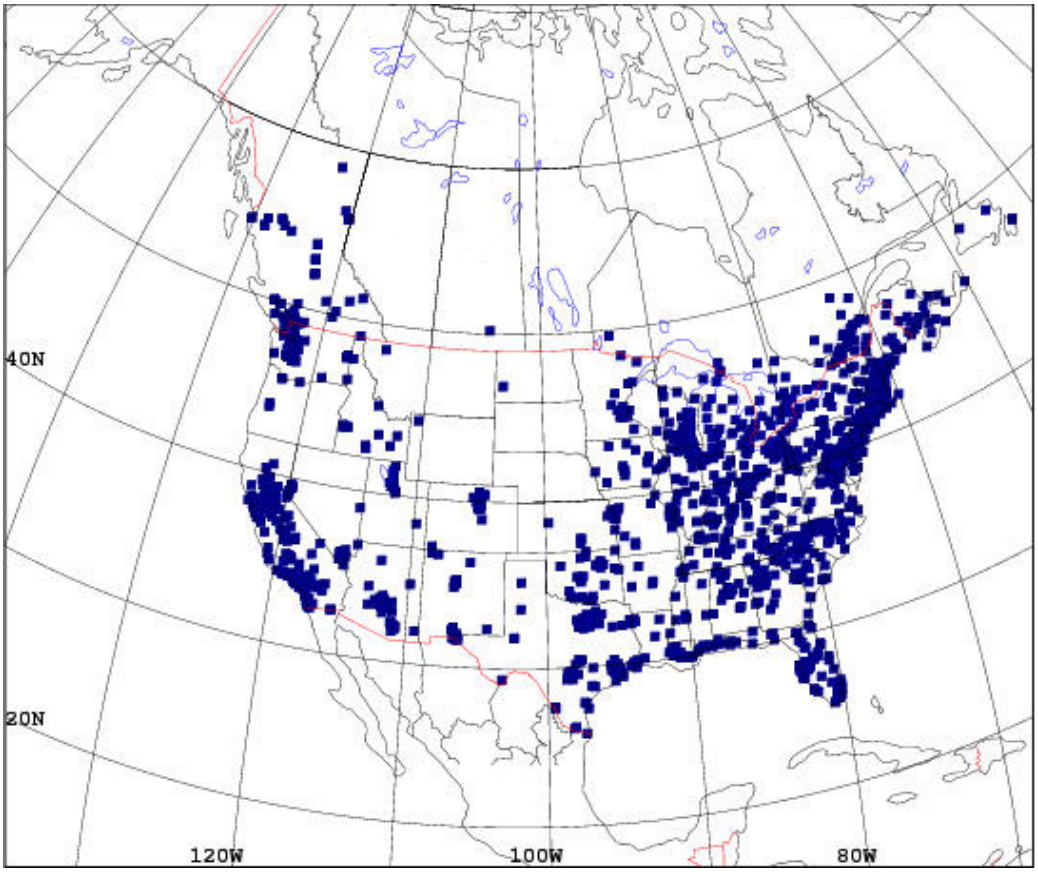

FIGURE 1. Surface ozone stations in EPA-AIRNOW data base.

Data check is performed on a real-time basis to remove outliers. Automatic quality control (QC– level 1) consists of a procedure to remove gross error and replace them by a flag (usually -980). Missing data are labeled with a -999 flag.

In developmental mode, necessary calculations to produce OA were done on a LINUX work station using MATLAB to generate the increment analysis and for cross-validation calculation, SAS[2] for error statistics calculation; TCL[3] scripts and SPI[4] for graphics and outputs. In operational mode, calculations uses TCL and UNIX scripts to collect all information required to assemble data whereas a FORTRAN 90 program calculates the O-P field. The field is added up to the trial field with and put on the internal WEB page (http://iweb.cmc.ec.gc.ca/~afsgmof/CTM/CTMframe.html).

4) MODELLING CHRONOS ERROR STATISTICS

Description of CHRONOS model (V2.3.6)

[2] SAS : Statistical Analysis Software, Cary, N.C.
[3] TCL: tool command language
[4] SPI: Spherical Projection Interface, a software developed at CMC.

The Canadian Hemispheric and Regional Ozone and NOx System (CHRONOS) has been designed for the prediction of atmospheric oxidants on both regional and hemispheric scales. The original version of the system was described initially under the generic name of Chemical Transport Model (CTM) by Pudykiewicz et al. (1997).
The model is used for real-time forecasting of surface ozone and other pollutants. Main characteristics of the model are:
- meteorological driver: GEM (Global Environmental Multi-scale model, resolution 24 km),
- source of emissions: 1990 Canadian and U.S. inventories,
- advection scheme: positive-definite, nonoscillatory, semi-Lagrangian method,
- vertical diffusion: based on prognostic equation for TKE with the values of the vertical diffusion coefficient derived from GEM,
- gas-phase chemistry mechanism: ADOM-2 mechanism; 47 advected species,
- aerosol dynamics: sedimentation,
- cloud processes: cloud attenuation and enhancement photolysis rates based on ADOM algorithm,
- dry deposition: improved multiple resistance method (Robichaud et al., 2003; Zhang et al., 2002 for non-stomatal formulation),
- wet deposition: distribution of LWC is used to calculate the wet scavenging term by applying Sundqvist formulae for the rate of release precipitation,
- grid structure: rectangular mesh with typical dimension 350 X 250 X 20
- horizontal discretization: structured grid defined on polar steographic projection: resolution 21 km,
- vertical discretization: Gal Chen terrain-following coordinates (model top at 4 km)
-initialization and lateral boundary conditions: integration using spin up from arbitrarily specified initial conditions (no data assimilation); zero-gradient flow and open outflow boundary conditions.

Estimation of error statistics

The first step in building up an objective analysis is to estimate error statistics. That is the goal of this subsection. The estimation of error statistics is based on the hypothesis of homogeneity (same correlation function everywhere) and isotropy (correlation function which only depends on distance).

The technique of Hollingsworth and Lonnberg (1986) is adopted here. In this technique, one estimates the innovation at different locations for different time of the day and different seasons. Hence, for a given observing station we report on the vertical coordinate the variance of innovation for that station. On the other hand, we also plot on the same graph the covariance of innovation with other stations as a function of the distance between the reference station and other stations (figure 2). We then take the average of covariance in bins of 30 km width and then fit the result with a FOAR curve (First Order Autoregressive Model) which is simply an exponential of the type b0*exp(b1*d) where d, is the distance, b0, the value of the covariance of innovation. At zero distance (intercept), the latter turns out to be the “pure model error” at the reference station. Finally, b1 is the inverse of what we call the “ correlation length ”. This is the distance where the innovation covariance falls by a factor of 1/e of the value of the covariance at zero distance. It was found in this report that the covariance error for a given station better follows a FOAR model (First Order Auto Regressive) rather than a SOAR (Second Order Auto-regressive Model) or TOAR (Third Order Auto-regressive Model) fittings usually adopted for meteorological fields (Gauthier et

al., 1999; Mitchell et al., 1996). According to turbulence theoretical arguments for a **tracer**, FOAR modeling has a lower sum of square errors than that of any other function (SOAR or TOAR). Note that when the contribution of advection is strong and that of photochemical processes weak, surface ozone can be considered as a tracer.

Figure 2 is equivalent to a variogram of model departure (or innovation) covariances stratified against distance. At zero distance, the variogram provides averaged information about the "intrinsic" model error for a given reporting station and the observation error (Courtier et Bouttier, 2000) and we have:

$$\mathbf{Var}\,(y^o - HX^b)_k = \mathbf{R}_k^2 + \mathbf{HP^fH^t}_k \qquad (7)$$

or

$$\textbf{Total variance} = \textbf{Obs. Error} + \textbf{Model Error.}$$

The term on the left of (7) is obtained by substraction of model value from observations. The second term on right hand side of (7) is obtained from the variogram of figure 2 (intercept of FOAR fit). Therefore, the first term on the right hand side of (7) is easily deduced and evaluation of A matrix and equation 2 are now possible. Variograms must be constructed for each reporting station k at different time of the day and for different seasons. Reporting stations where no variogram could be obtained are thought to be spatially non representative or non-correlated with nearby stations. How to treat those cases in an assimilation system is still not clear and more research is needed on that aspect. Figure 2 also shows that innovation covariance vanishes as great distance as it should be. In most cases, the background error covariances should go to zero for very large distance. If this is not the case, it is usually the sign of biases in the background and/or the observations and the method may not work correctly (Hollingsworth and Lonnberg, 1986). For example, having covariance of innovation constant with distance would mean that the radius of influence of a particular data does not decrease with distance which is obviously non-physical (being associated then with infinite correlation length). Estimation technique used here shows that typical correlation length varies from 100 to 300 km for surface ozone. Note that in order to simplify the approach, the correlation length will be taken as a constant over the whole domain in the rest of this report.

The procedure NLIN of SAS/STAT[5] (Newton method) was used for the non-linear fitting. Quality control was developed to filter out inappropriate curve fittings (see section 5).

[5] SAS/STAT: Statistical Analysis Software, SAS/STATS User's Guide, Relese 6.03 Edition, Cary, NC, 1998.

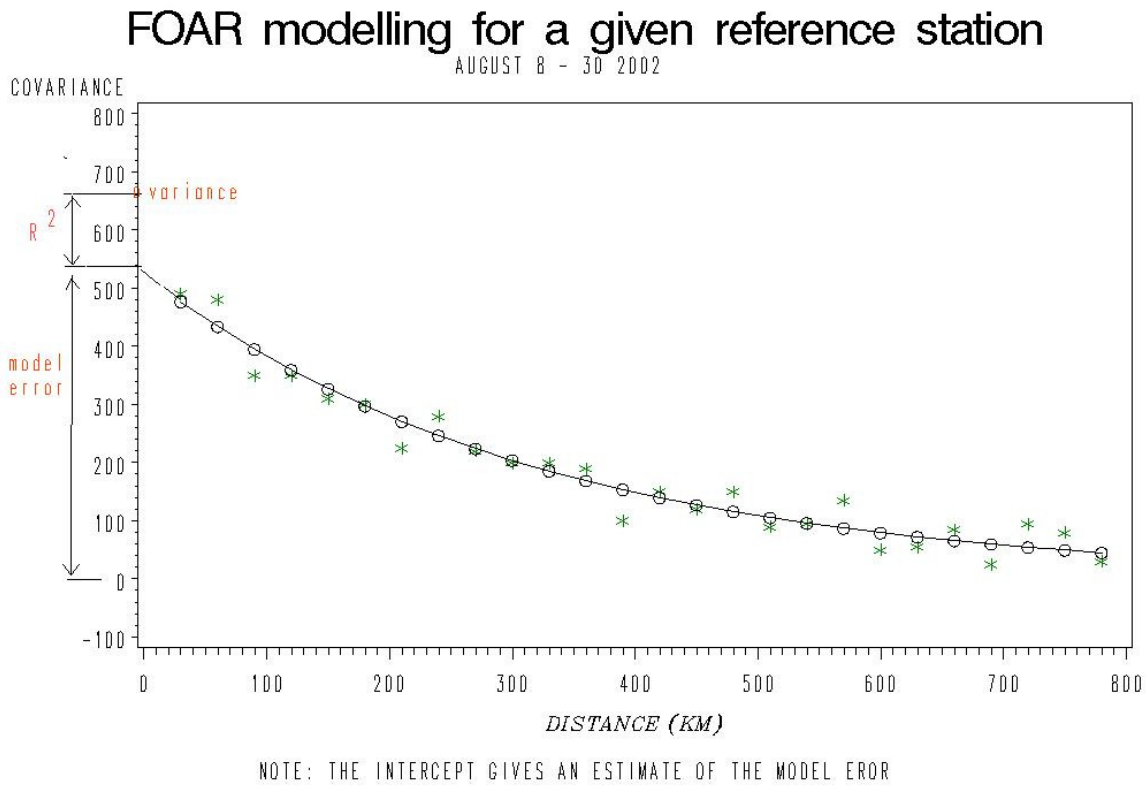

Figure 2. Estimation of error statistics.

MAPPING "INTRINSIC" CHRONOS MODEL ERROR

Using the ideas developed above, a spatial mapping of model error statistics obtained from FOAR fittings was performed. Figure 3a,3b,3c and 3d respectively show a map of the variance of innovation for all reporting stations in the EPA-AIRNOW data base in August 2002 for a) 12Z, b) 18Z, c) 00Z and d) 06Z. Inspection of those figures reveal that the variance tends to be higher where the bulk of anthropogenic emissions is located (Eastern US and Southern California, see figure 9 for distribution of NOx emissions in NA). Similar conclusions can be reached for the field of model error, figure 4, for the same time a) 12Z, b) 18Z, c) 00Z and d) 06Z. Note that the model error here is considered as " pure model error " or " intrinsic model error " since it is obtained by the technique of FOAR modelling described above which allows to break down the error variance as two parts; 1) model error variance (σ_f^2) and 2) observation error, R^2, (instrument error and interpolation[6] error). Finally, the bias of a model is important to know since one of the fundamental assumption in the theory of statistical interpolation is that the bias be small at least compared to the

[6]Interpolation error can also be view as representativeness error

standard deviation of model error. Figure 5 shows model bias at a) 12Z, b) 18Z, c) 00Z, d) 06Z. Note an interesting diurnal cycle for bias. Overnight, most places show not much of underprediction (red color) or overprediction (blue color) whereas in the afternoon (most of Eastern US and California show significant overprediction).

(see following pages for those figures)

Figure 3.Total variance error at a) 12Z, b) 18Z, c) 00Z, d) 06Z
Figure 4. Model error at a) 12Z, b) 18Z, c) 00Z, d) 06Z
Figure 5. Bias at a) 12Z, b) 18Z, c) 00Z, d) 06Z
CHRONOS V2.3.3, Aug 8-30 2002 interpolated in the observation space.

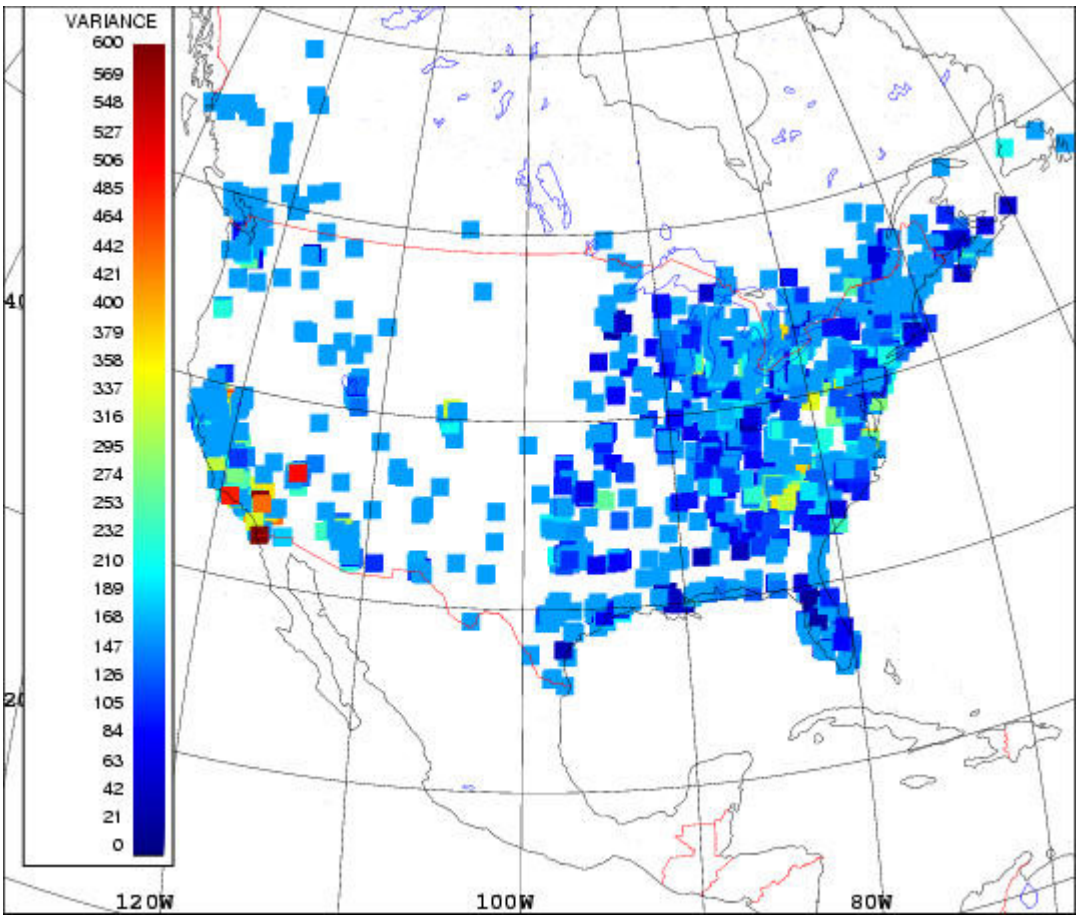

FIGURE 3A. 12Z.

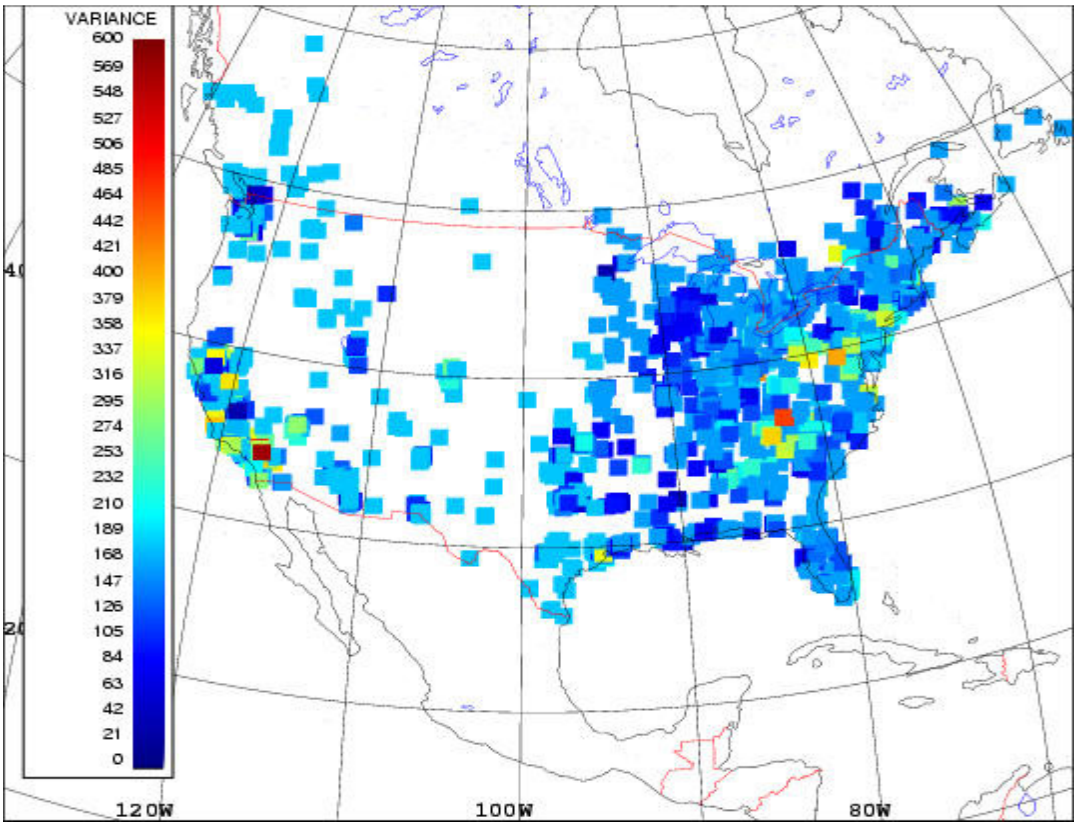

FIGURE 3B. 18Z.

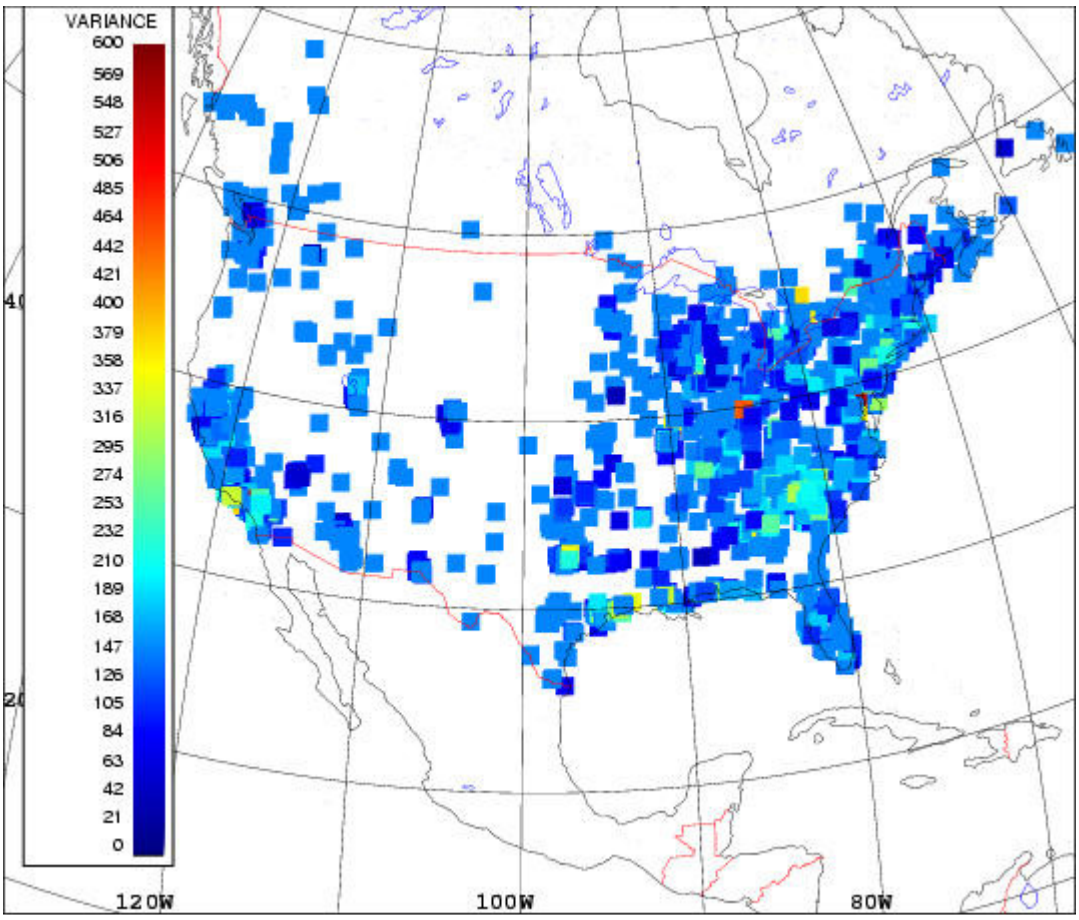

FIGURE 3C. 00Z.

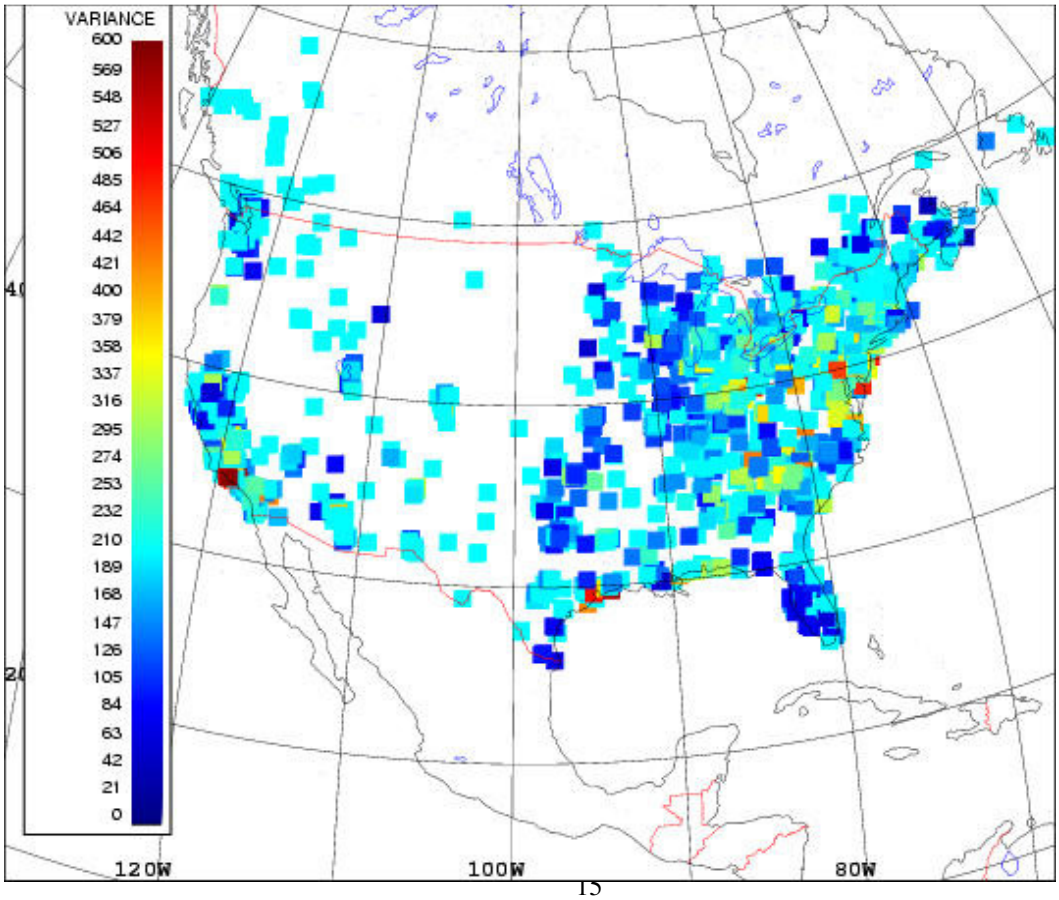

FIGURE 3D. 06Z.

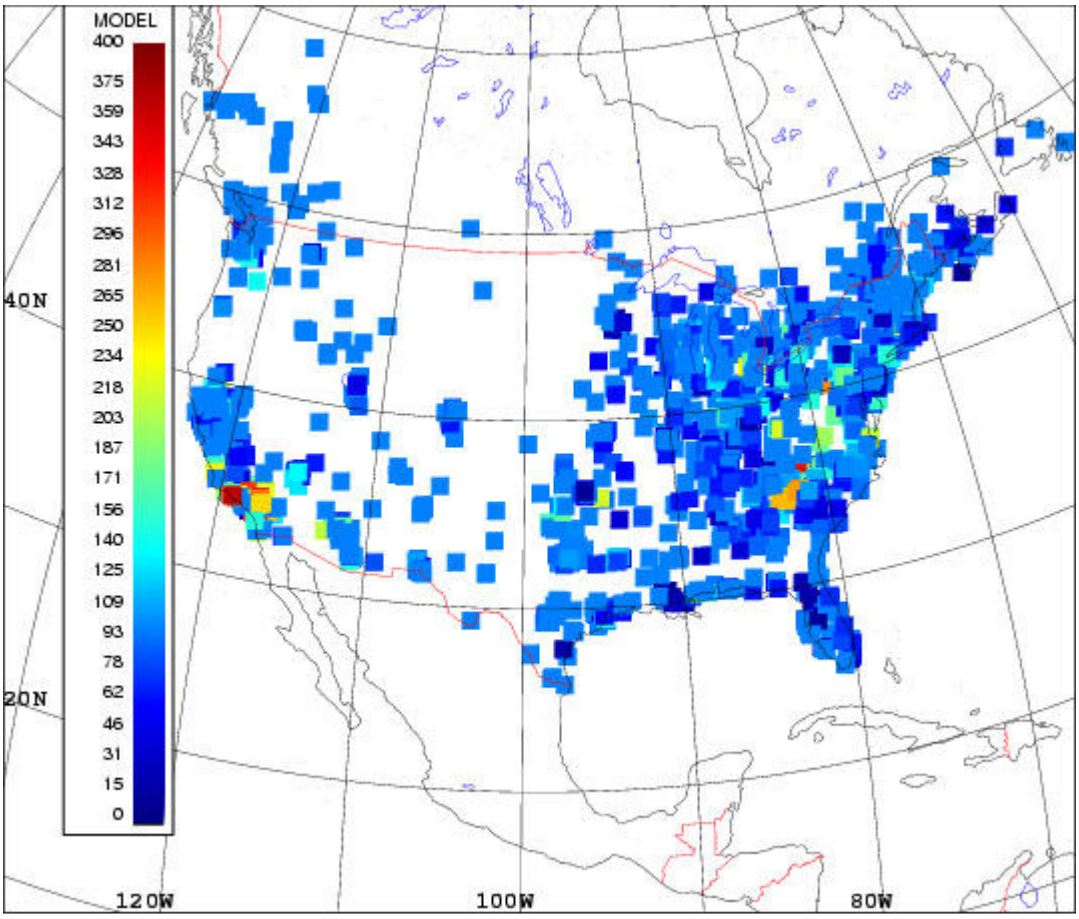

FIGURE 4A. 12Z.

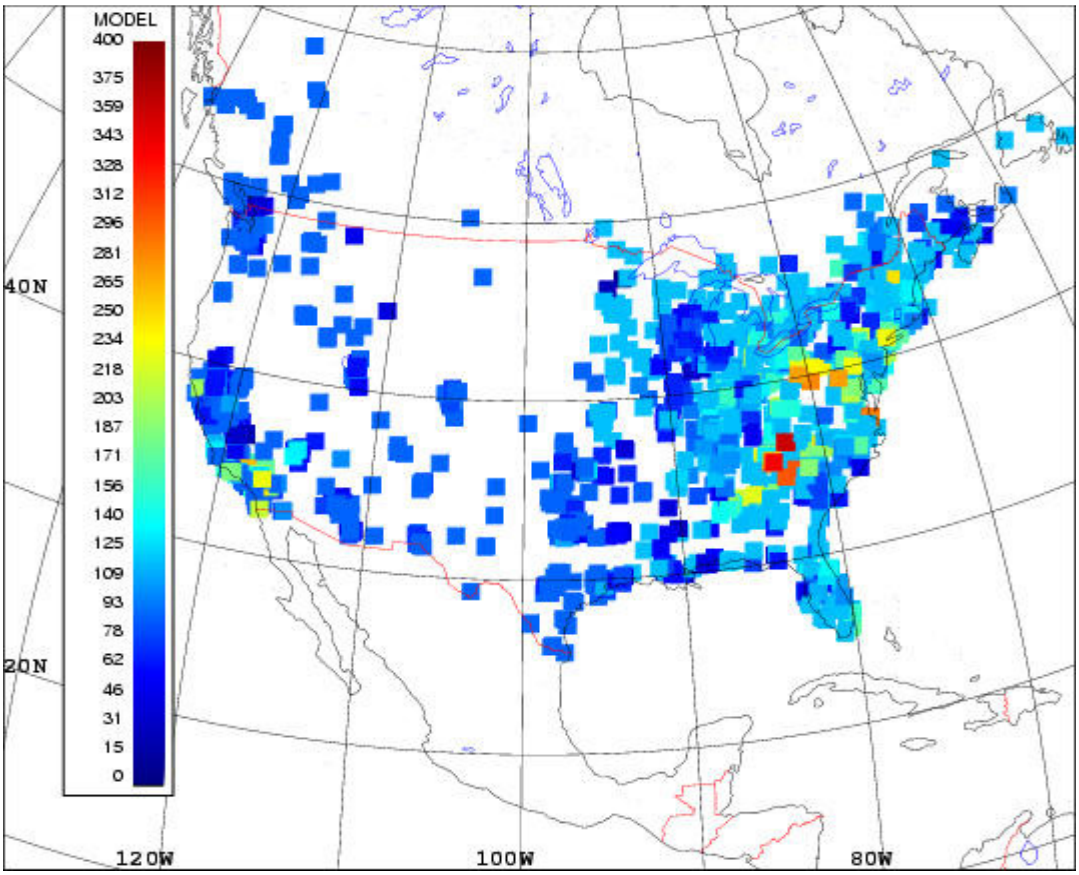

FIGUIRE 4B. 18Z.

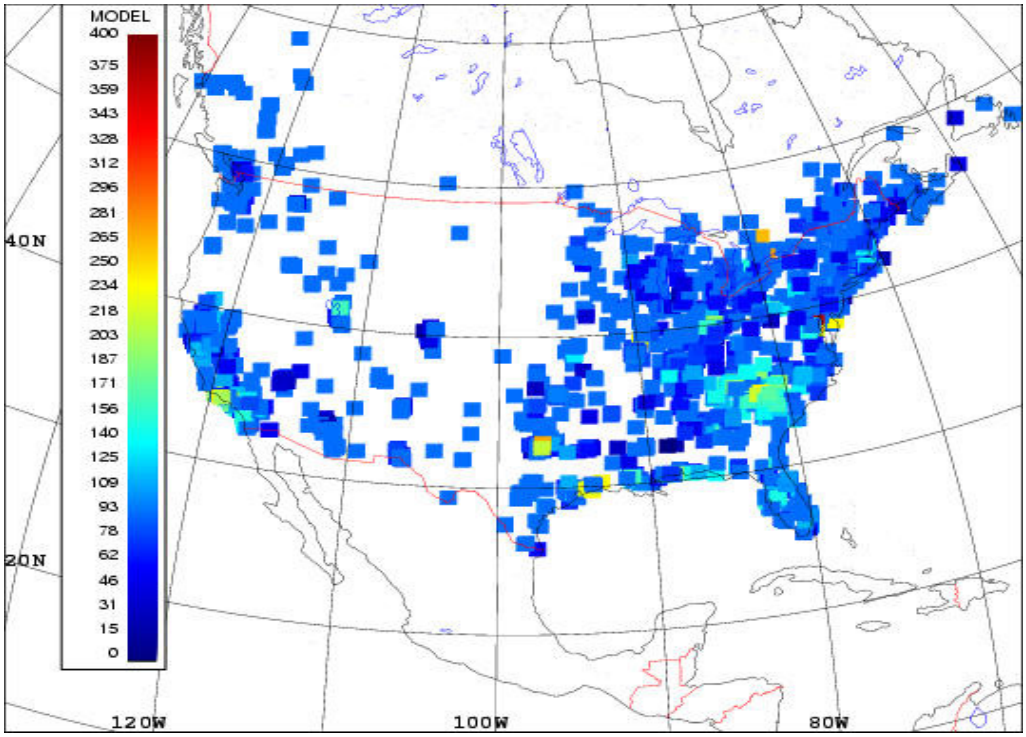

FIGURE 4C. 00Z.

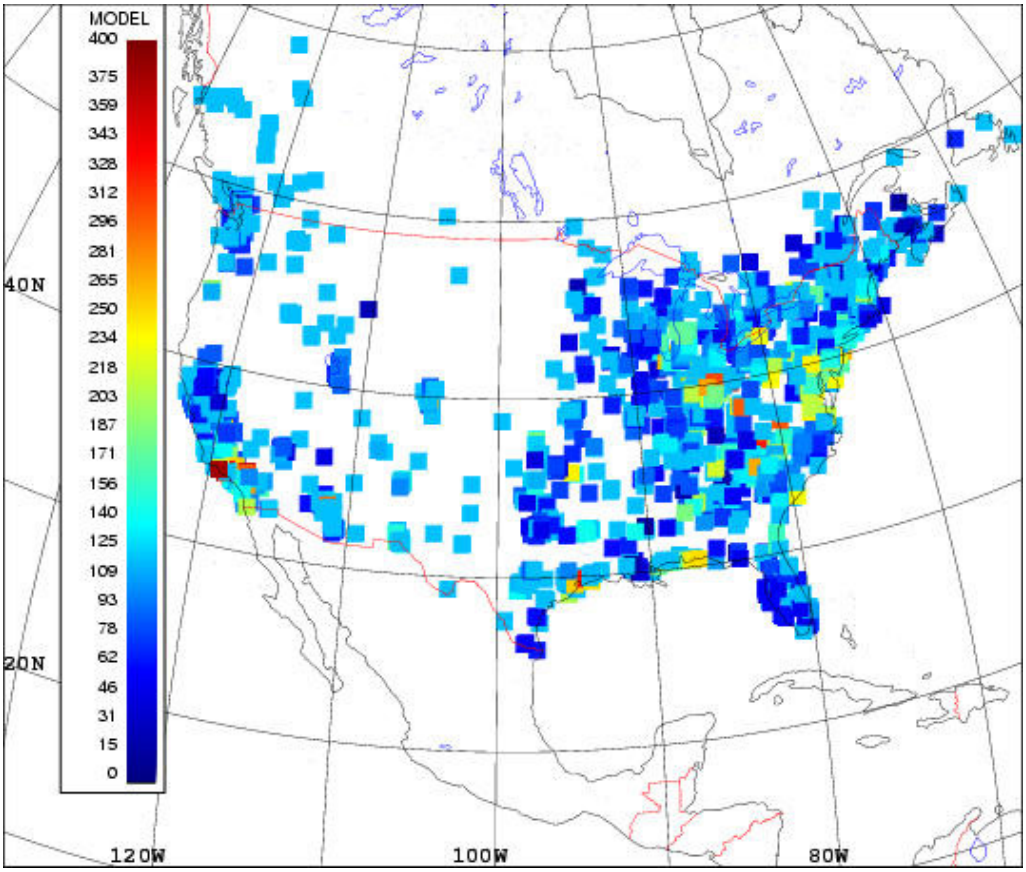

FIGURE 4D. 06Z.

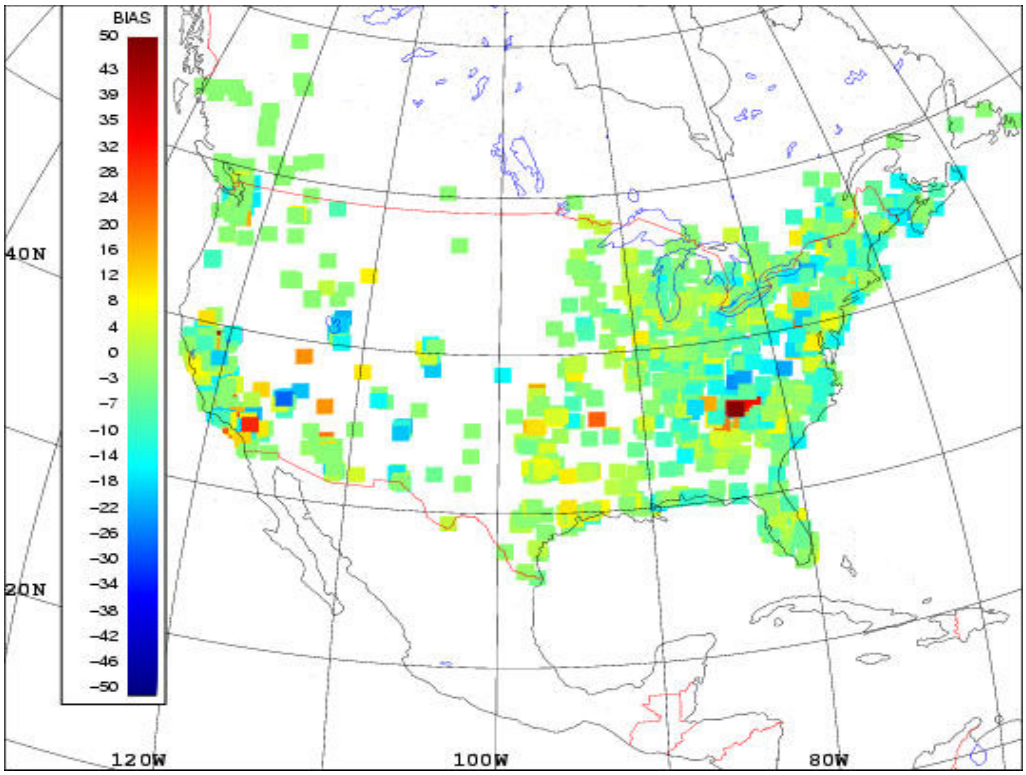

FIGURE 5A. 12Z.

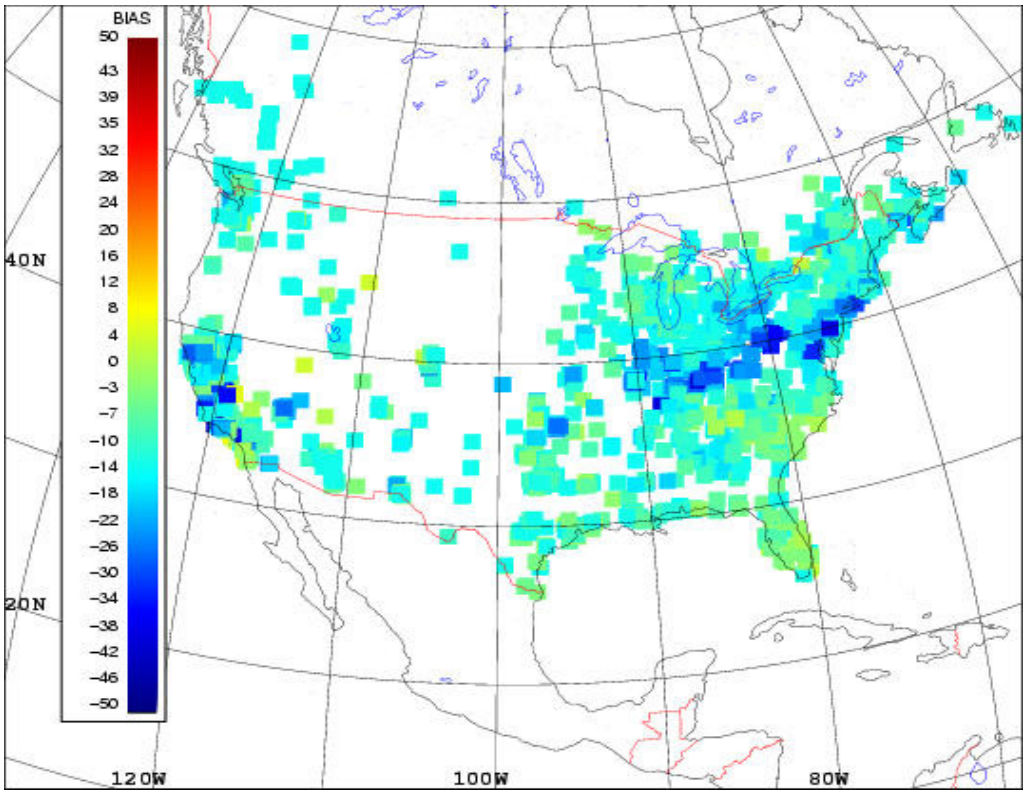

FIGURE 5B. 18Z.

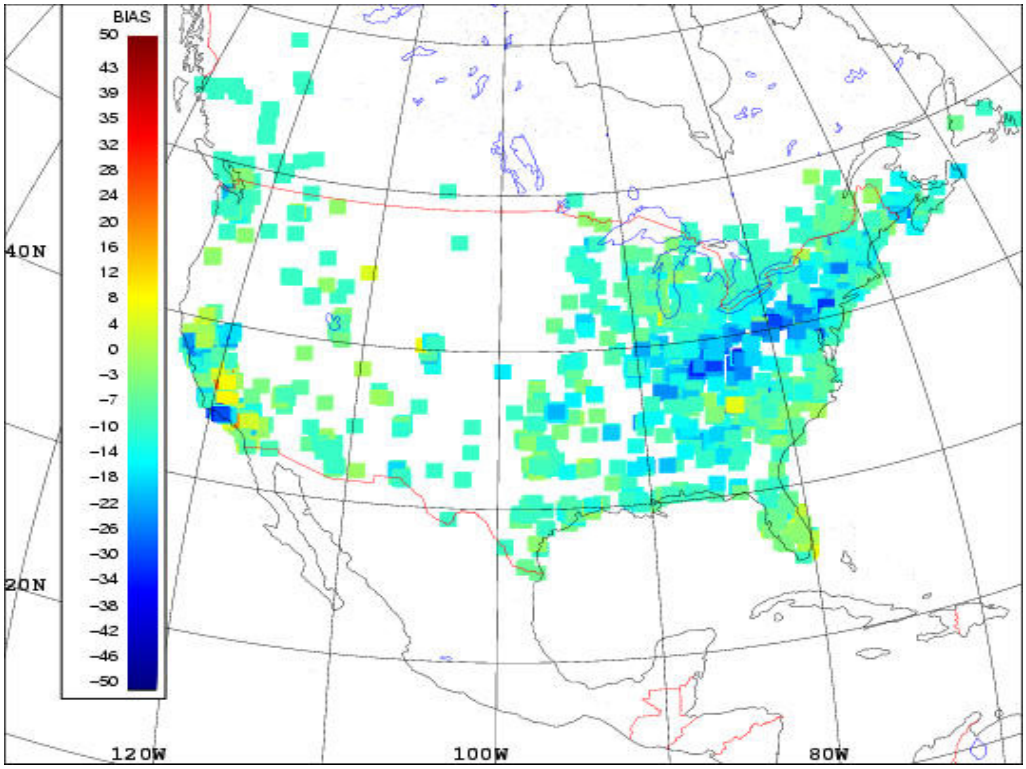

FIGURE 5C. 00Z.

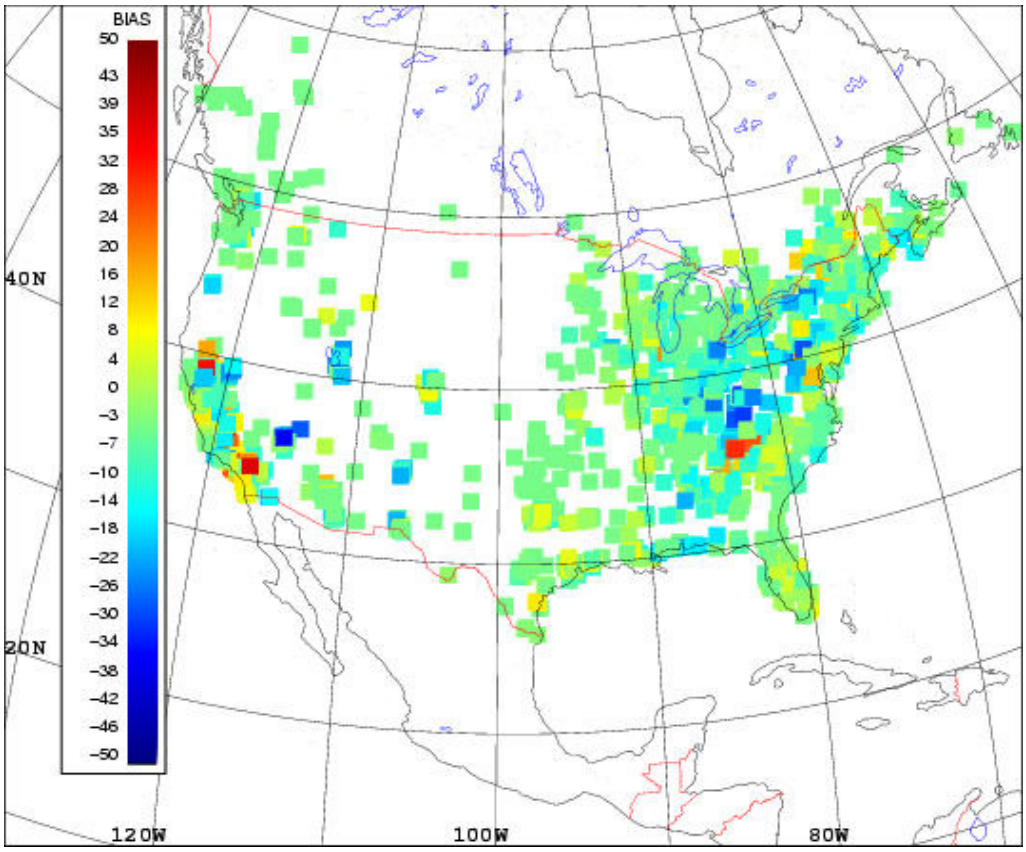

FIGURE 5D. 06Z.

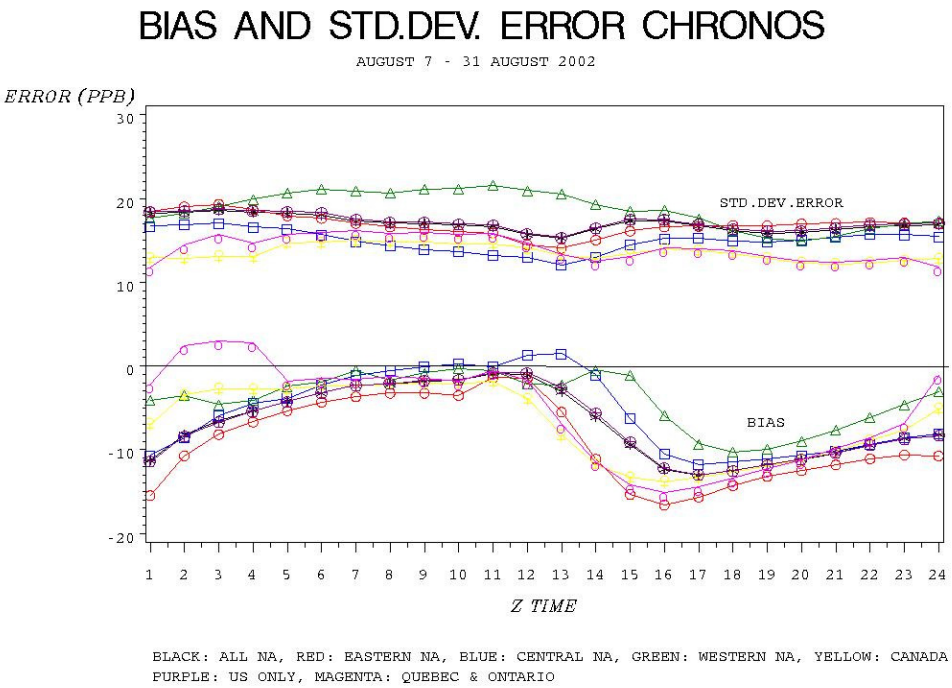

FIGURE 6. Diurnal behavior of CHRONOS model error bias (bias = obs – model) and standard deviation of error by regions (NA: North America).

Figure 6 confirms that Chronos model overpredicts for all regions of North America particularly near midday (around 16Z). It is clear that a strong diurnal bias cycle exists as far as the CHRONOS model is concerned. However, the standard deviation of error only shows a weak diurnal cycle varying from about 12 to about 21 ppb. At night, it tends to vary from one region to another more than during the day. In Canada, or Quebec&Ontario regions, the standard deviation of error is usually less than other regions as expected since less anthropogenic sources are present as compared to Eastern US for example..

It is also relevant to look at frequency distribution of innovation or model error. Figures 7 a),b),c) and d) show those distribution for 4 times of the day: 8,12,16 and 20 EDT time (or 12,16,20 and 00Z). Those distributions tend to be Gaussian centered around zero at night (figures 7A and 7D) and almost Gaussian but not centered to zero during the day (figures 7B and 7C). This is an important verification to do since one of the main hypothesis of the theoretical framework of this theory is that model error distribution are Gaussian centered to zero. However, the theory still works even if this criteria is not met but may or may not produce an “optimal” OA. Nevertheless, this aspect is not clear and is considered as a research topic.

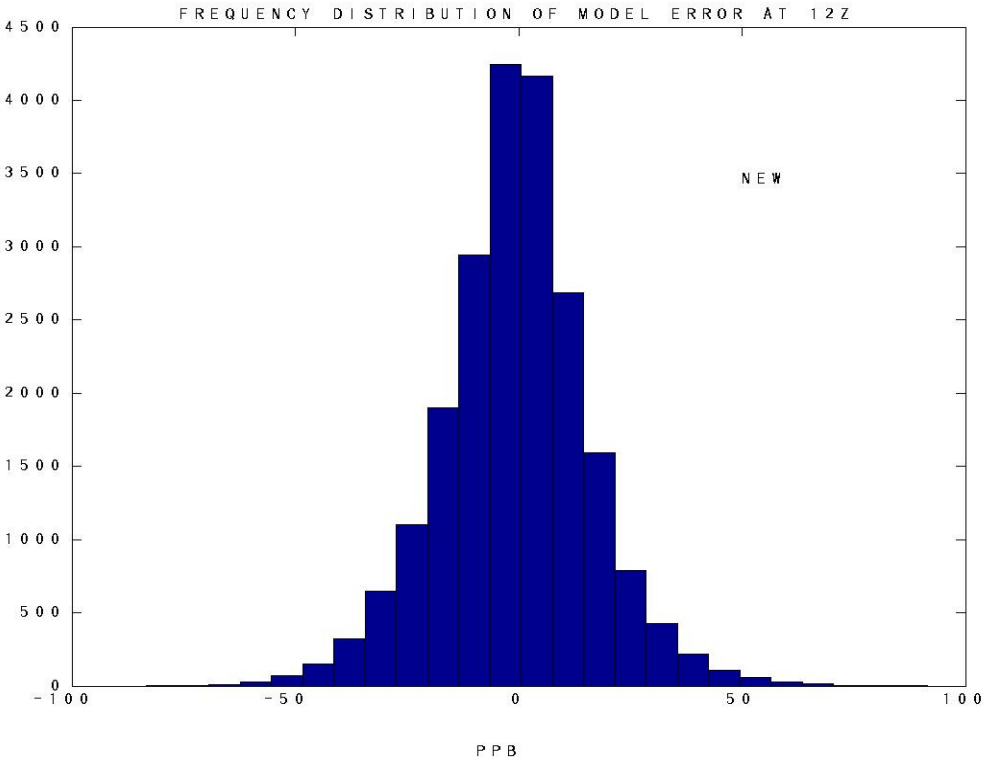

FIGURE 7A.

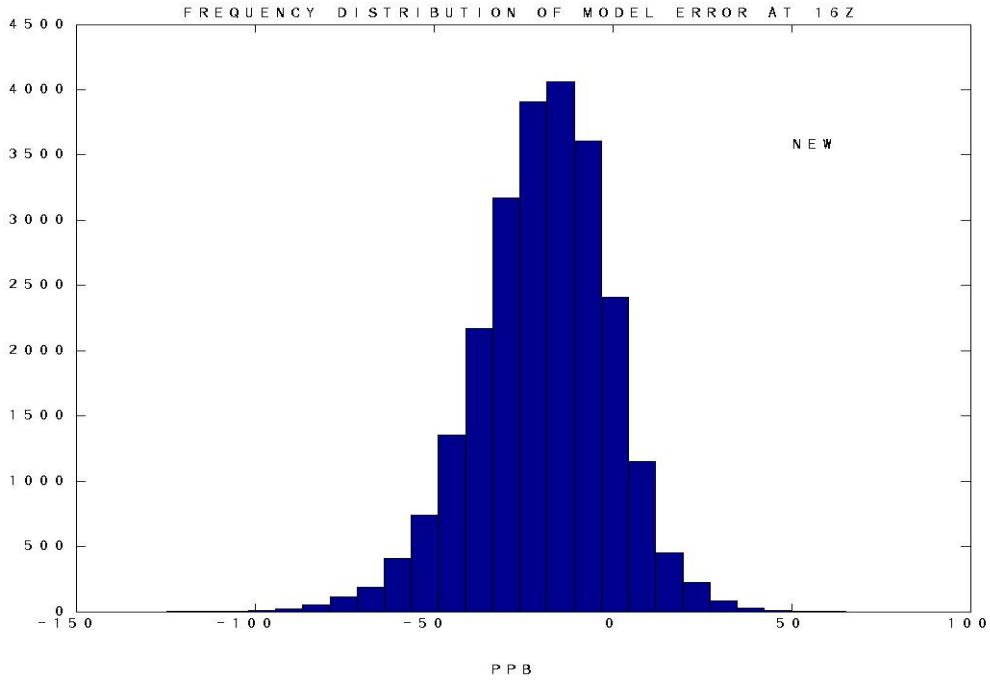

FIGURE 7B.

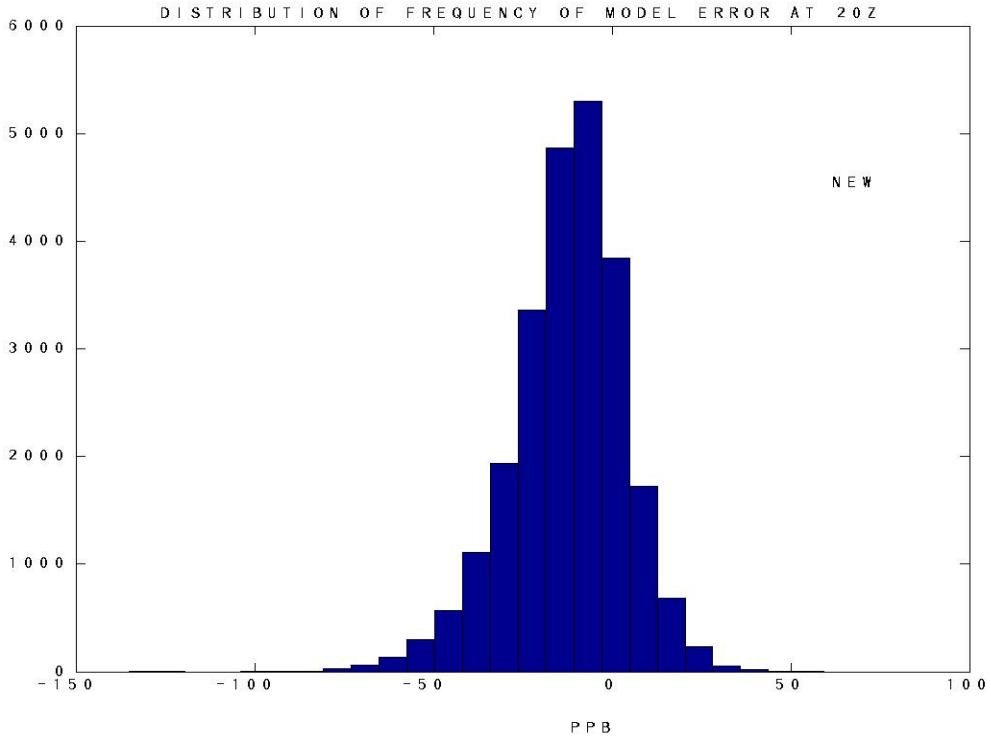

FIGURE 7C.

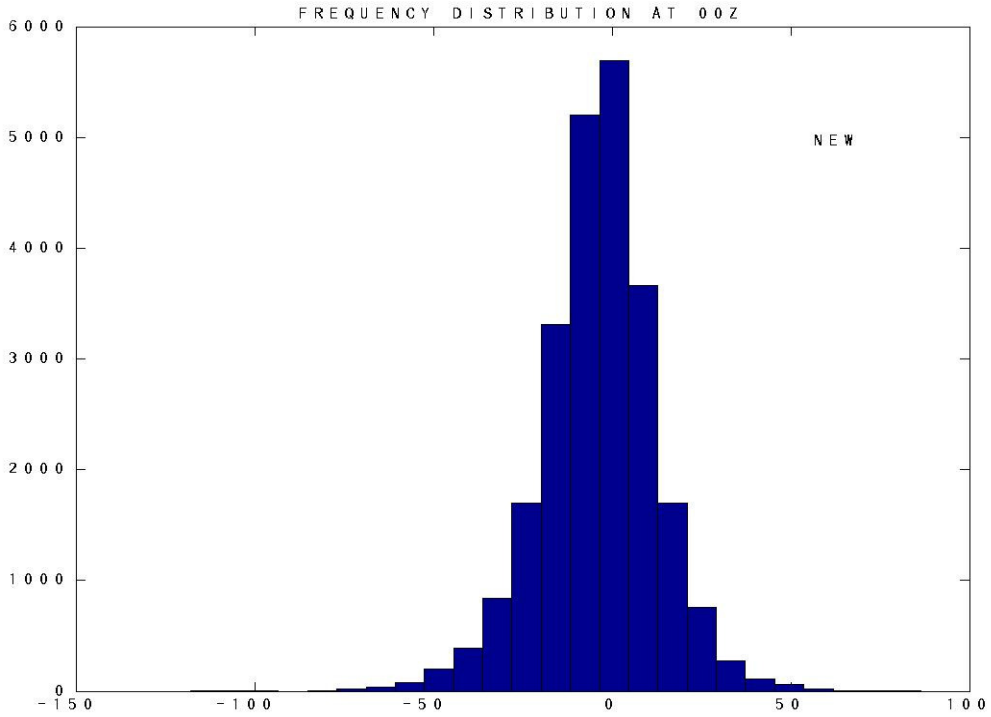

FIGURE 7D

5) QUALITY CONTROL OF OBJECTIVE ANALYSIS

The quality control is performed at different levels; 1) for error statistics (off-line), 2) for real-time innovation and for output of final OA maps (on-line).

- Error statistics

Error statistics are not calculated in real-time but prior to an OA experiment[7]. They remain constant for a given station during a given time of the day or during a given season. The quality control is performed so that data is rejected if:

1) intercept (i.e model error) > variance of innovation
2) intercept < 0 (i.e negative "intrinsic" model error)
3) correlation length is less than 20 or greater than 2000 km

In any of those cases, the rejected values could be replaced by mean values obtained from average over the whole domain of other stations having valid data.

- **Real-time innovation**

When real-time innovation are calculated, reporting station data is rejected if

1) the absolute value of innovation is greater than 100 ppb
2) the interpolated value of model at observation location is less than zero (this is possible whenever Cubic Lagrangian interpolator is used)
3) the observation value is less than zero (due to missing or bad observation[8])

- **Output products** (Incremental analysis map and final map for OA)

In increment calculations, it is possible that a negative analysis increment (second term to the right hand side of equation (1)) be so big and negative that it gives a negative value in the OA field (X_a). In this case, the value of X_a is clipped to zero in the final map for OA, since negative values of pollutant concentrations are physically impossible. Finally, if the Chi-square diagnostic gives a value greater than 5, no OA map is produced since such a high value of Chi-square would indicate a major problem in the system (corrupted data or other bug). Note that in the incremental analysis map, white color would indicate a value outside the range (-50 to 50 ppb). This is a way to flag extremes values of increments in a real-time situation.

[7] To obtain error statistics which follows the real-time evolution of fields would require switching to the theory of Kalman filter.

[8] Usually the symbol for missing data is -999 and -980 for bad data

6) RESULTS

a) case study of July 21 2003 at 18Z

We give below the model output, observations, analysis increment and OA maps for July 21 2003 at 18Z as an example of a typical case obtained in a real time operational environment. High values of surface ozone were forecast in Eastern US that day as depicted in figure 8A. Observations (figure 8B) show lower values of ozone.

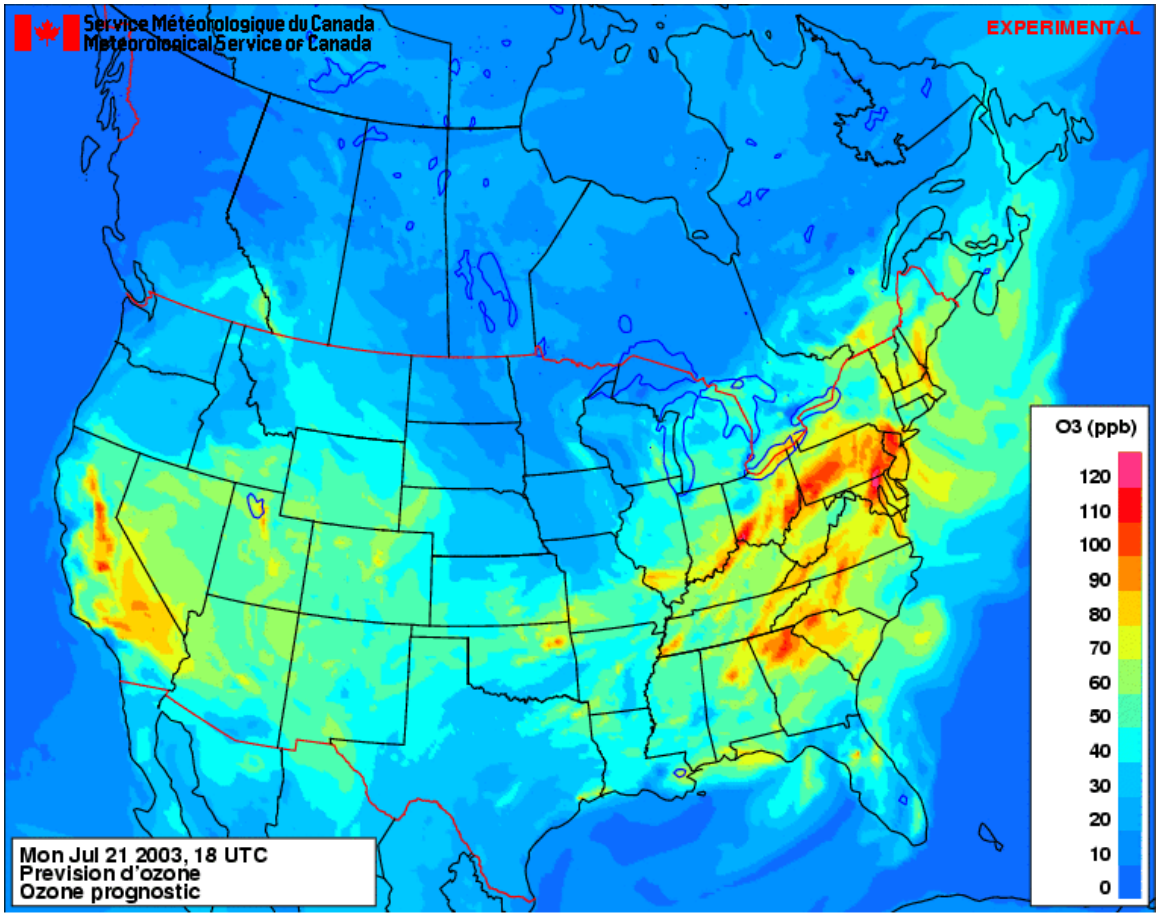

FIGURE 8A. BACKGROUND OR MODEL FIELD (X_b)

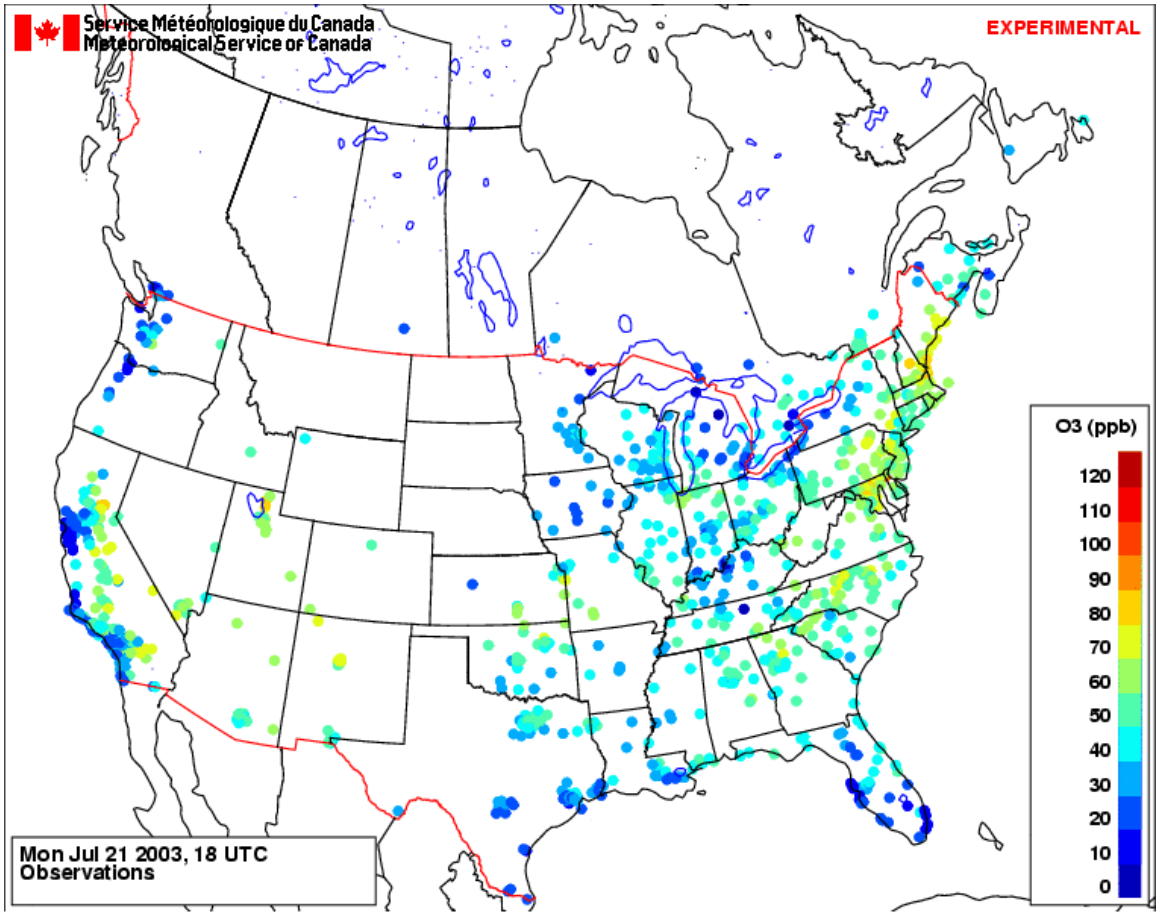

FIGURE 8B. OBSERVATIONS (y^o)

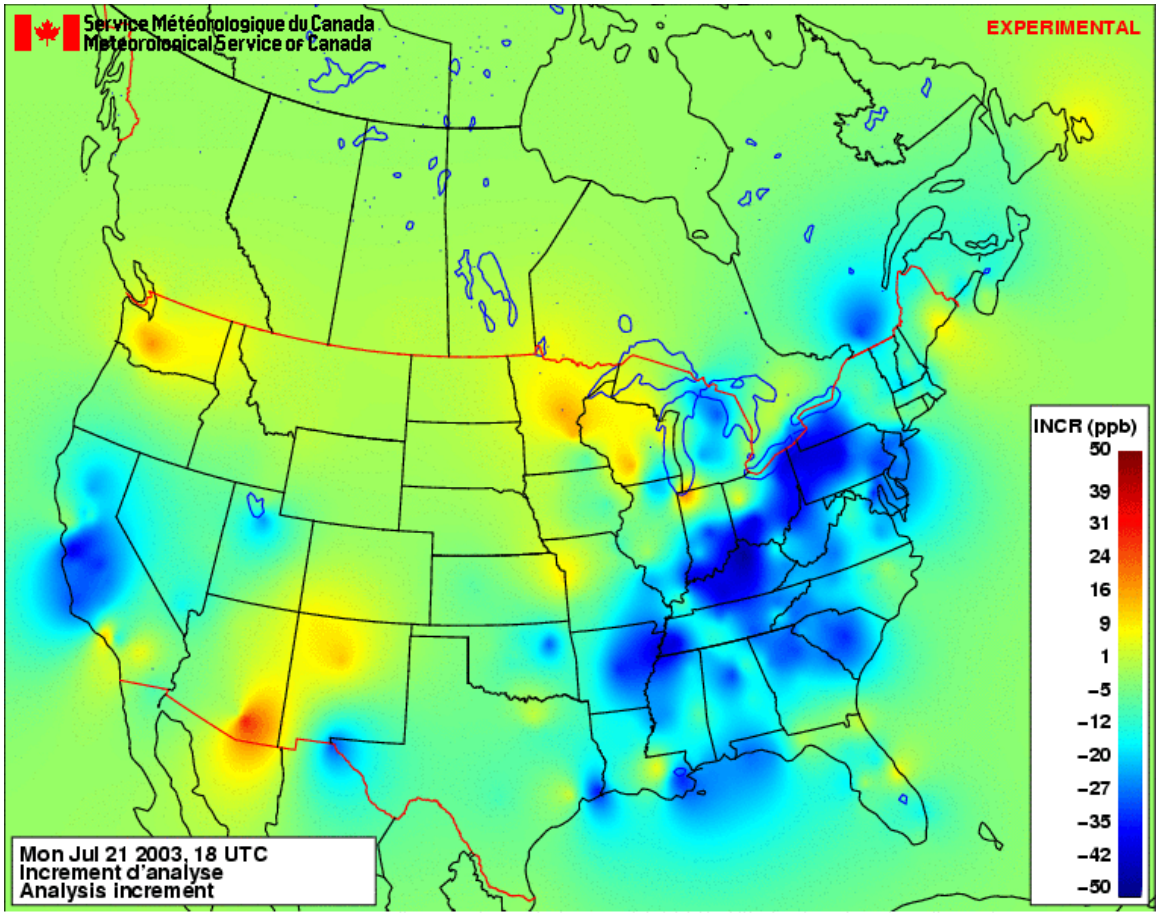

FIGURE 8C. ANALYSIS INCREMENT MAP

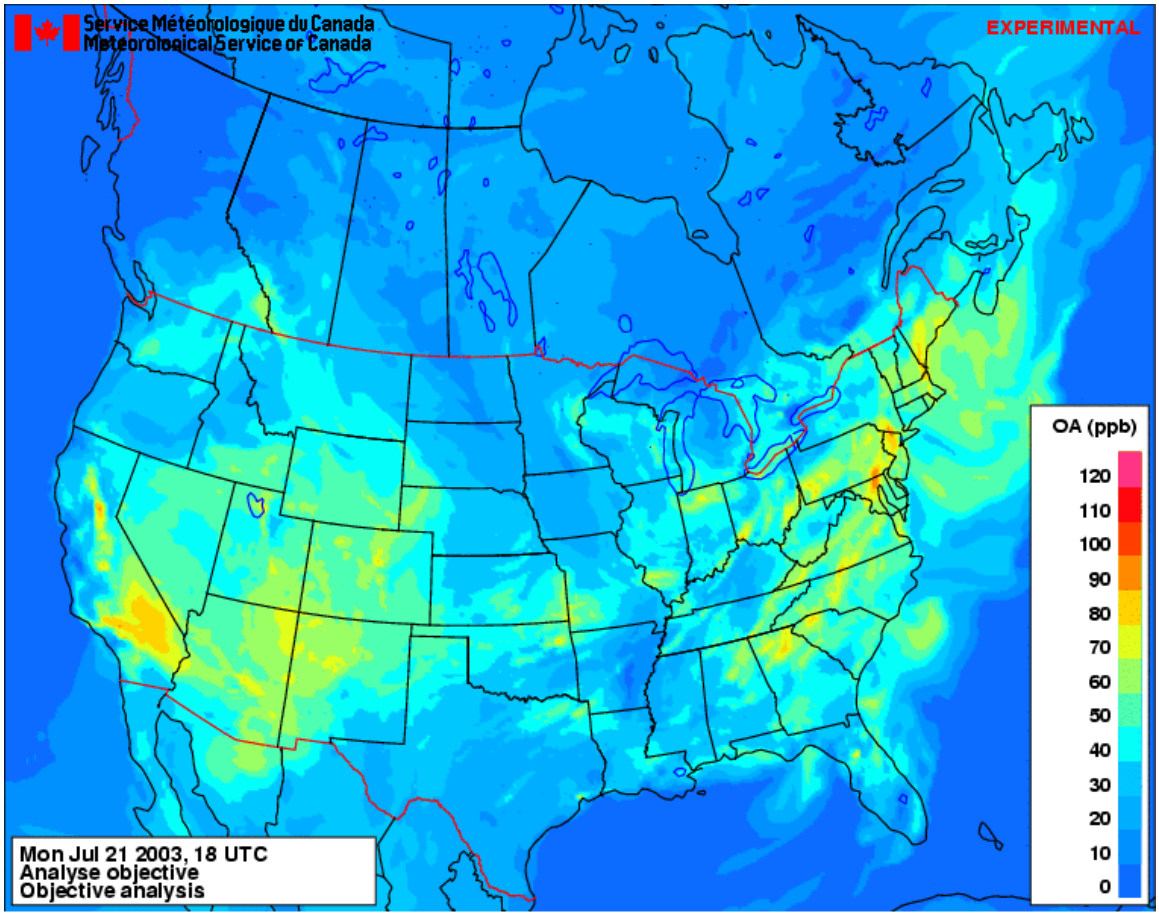

FIGURE 8D. OBJECTIVE ANALYSIS MAP (X_a)

Inspection of the above figures reveal that the model significantly overpredicts particularly over Eastern US and California. That is why analysis increments are strongly negative in those areas (figure 8c). The final OA map is obtained by adding analysis increments (figure 8c) to the trial field (figure 8a) to obtain figure 8d. Note that there is a broad link between the location of emission sources of ozone precursors (see figure 9 for NOx) and analysis increments (figure 8c) as anticipated. Scatter plots of model against observations and objective analysis against observations are shown in figure 10a) and b). Results show, as expected, dramatic improvement of the correlation coefficient (r^2 increases from 0.36 for X_b to 0.67 for X_a) and very significant reduction of RMSE for the regression fit. The mean bias (MB) is almost reduced to almost zero. The intercept of the fit is also significantly reduced with OA (X_a) as compared to that of the model (X_b).

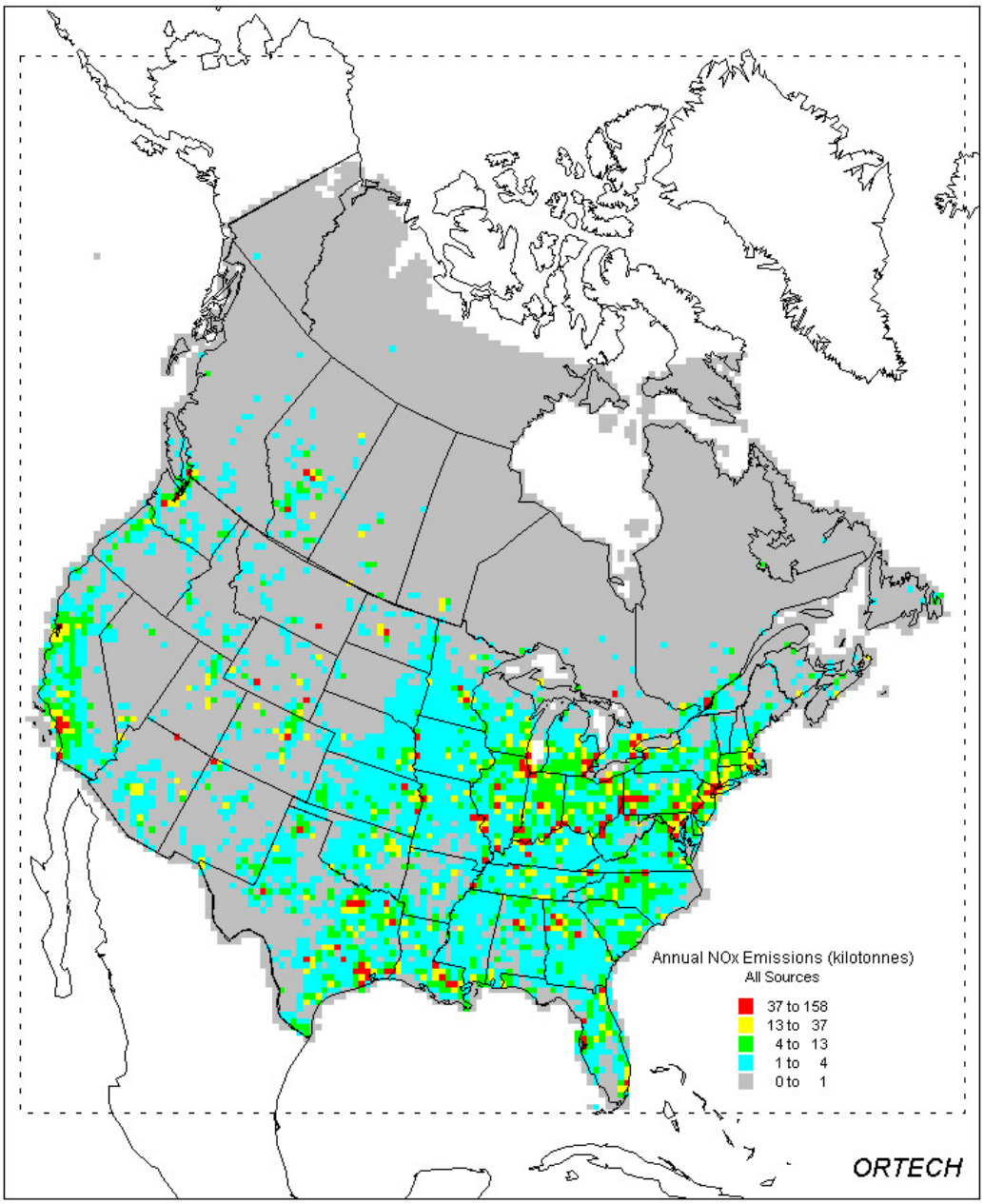

FIGURE 9. Location of major NOx sources in North America.

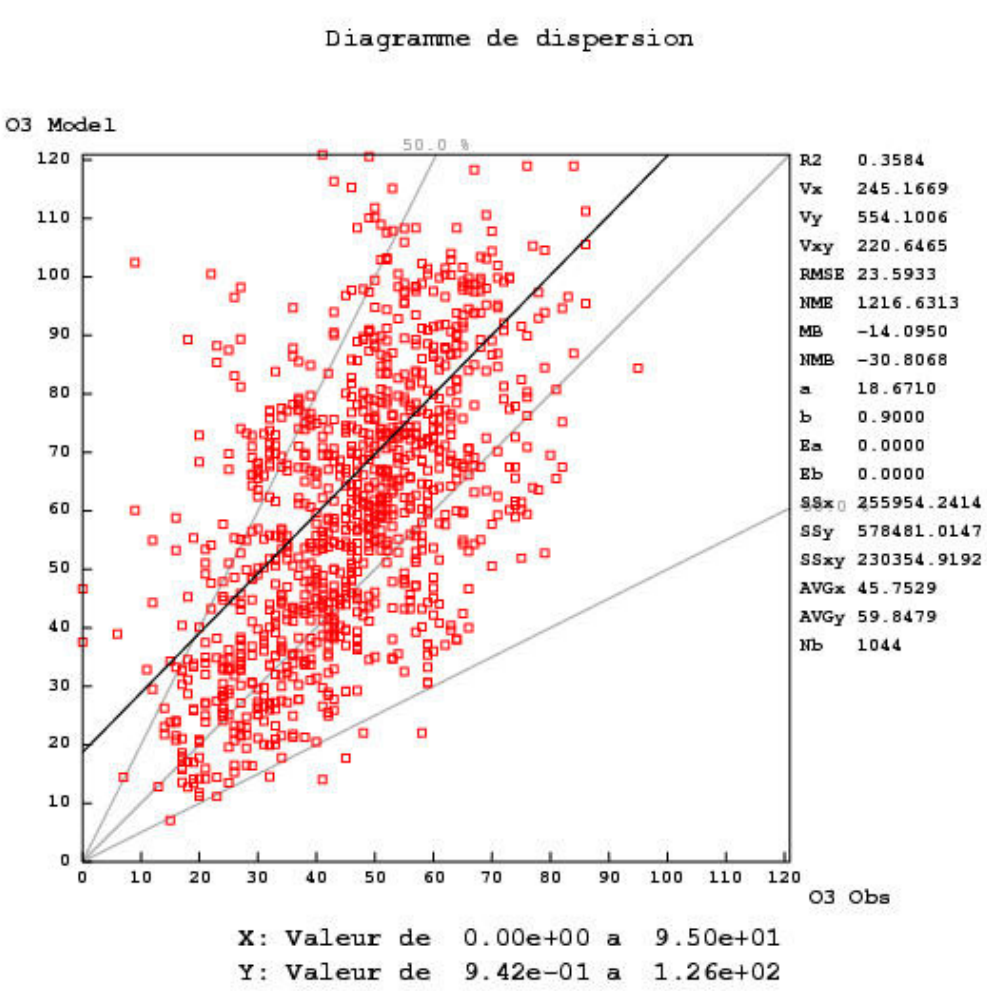

FIGURE 10A. Scatter plot and regression fit for X_b against observations for July 21 2003 at 18Z. The line 1:1 and 2:1 are also drawn in light gray color as reference.

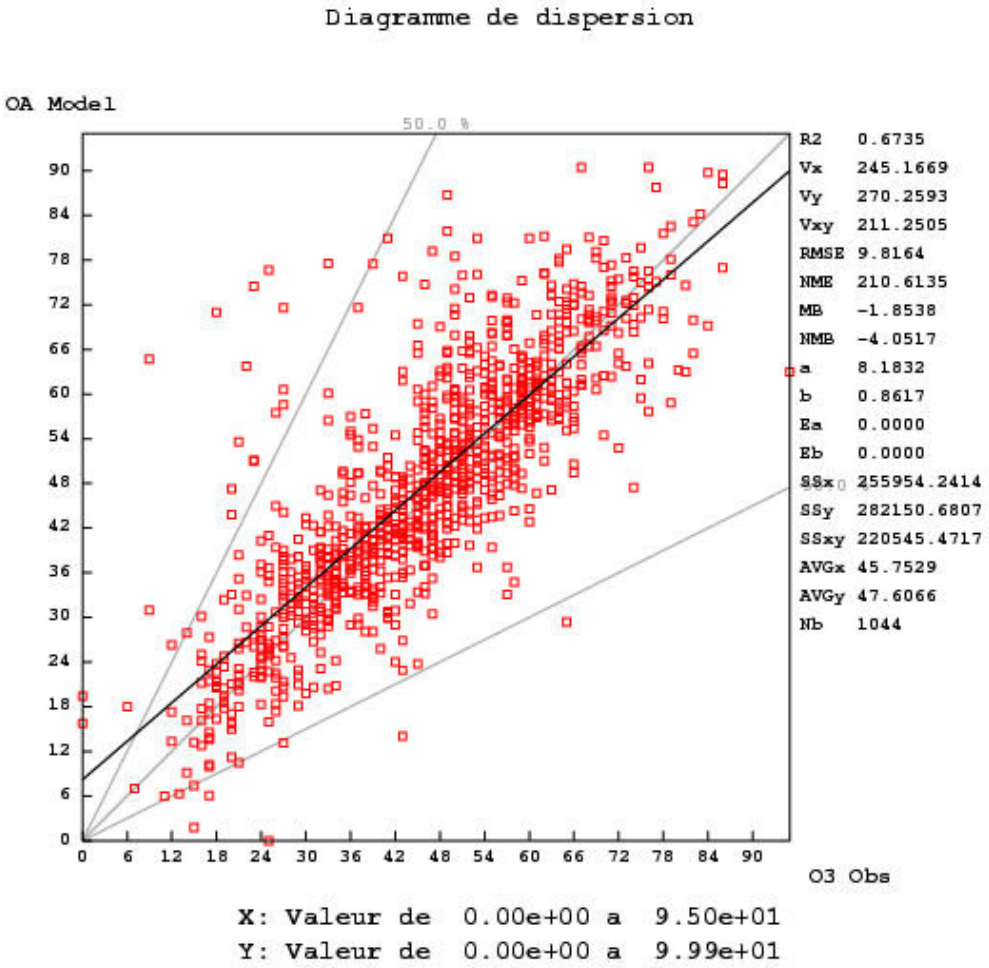

FIGURE 10B. Scatter plot and regression fit for X_a against observations for July 21 2003 at 18Z.

b) case study of July 31 at 20Z

As a second example, we show here the case of July 31st 2003 at 20Z which also shows high forecast values for ozone over Eastern US and California.

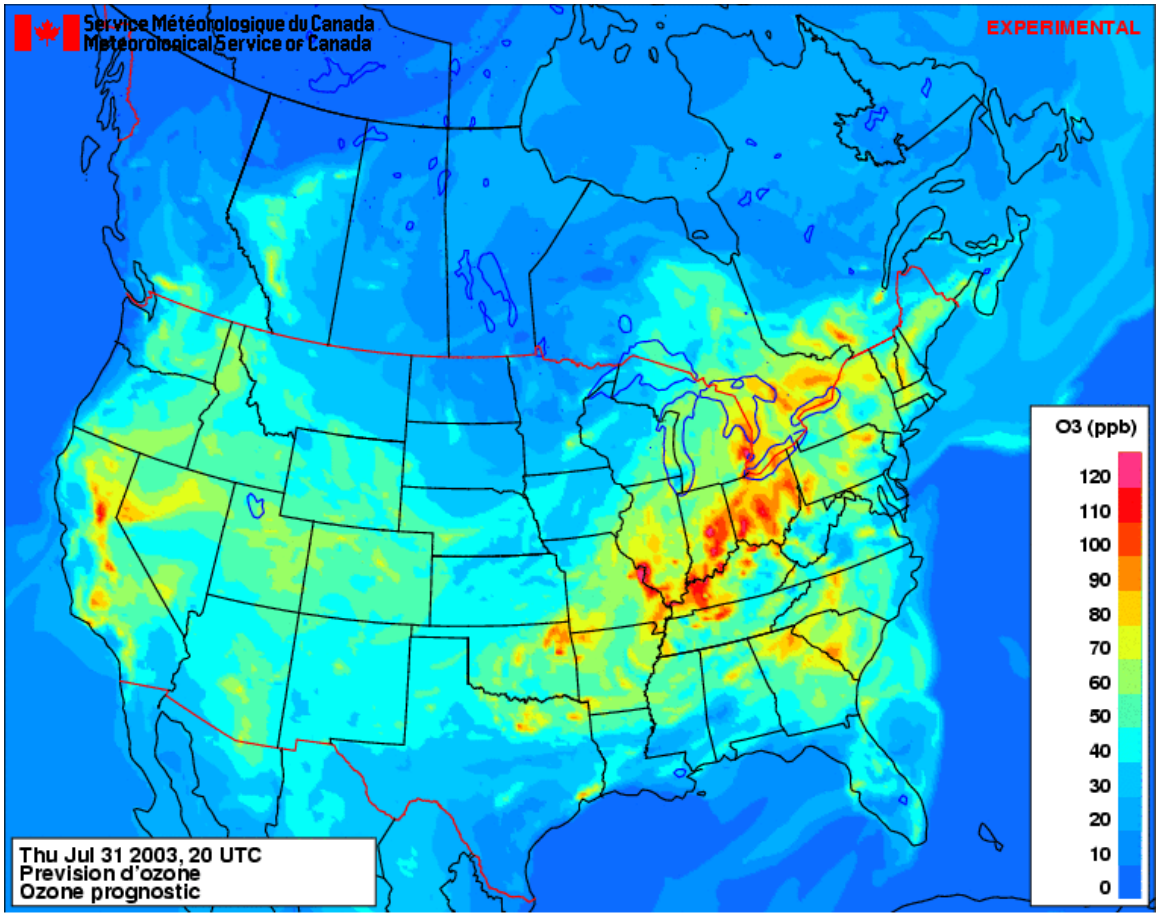

FIGURE 11A. Model output (X_b) for July 31, 2003 at 20Z.

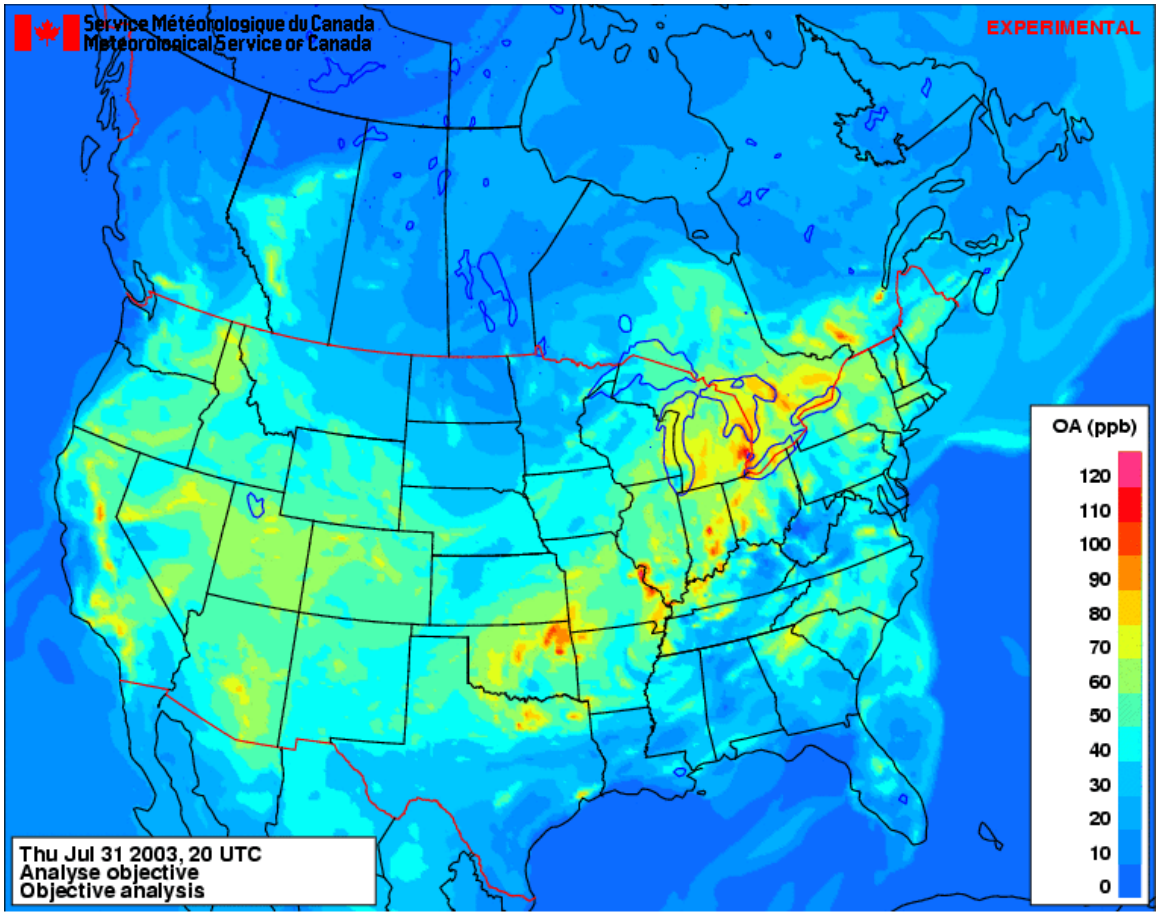

FIGURE 11B. OA output (X_a) for July 31, 2003 at 20Z.

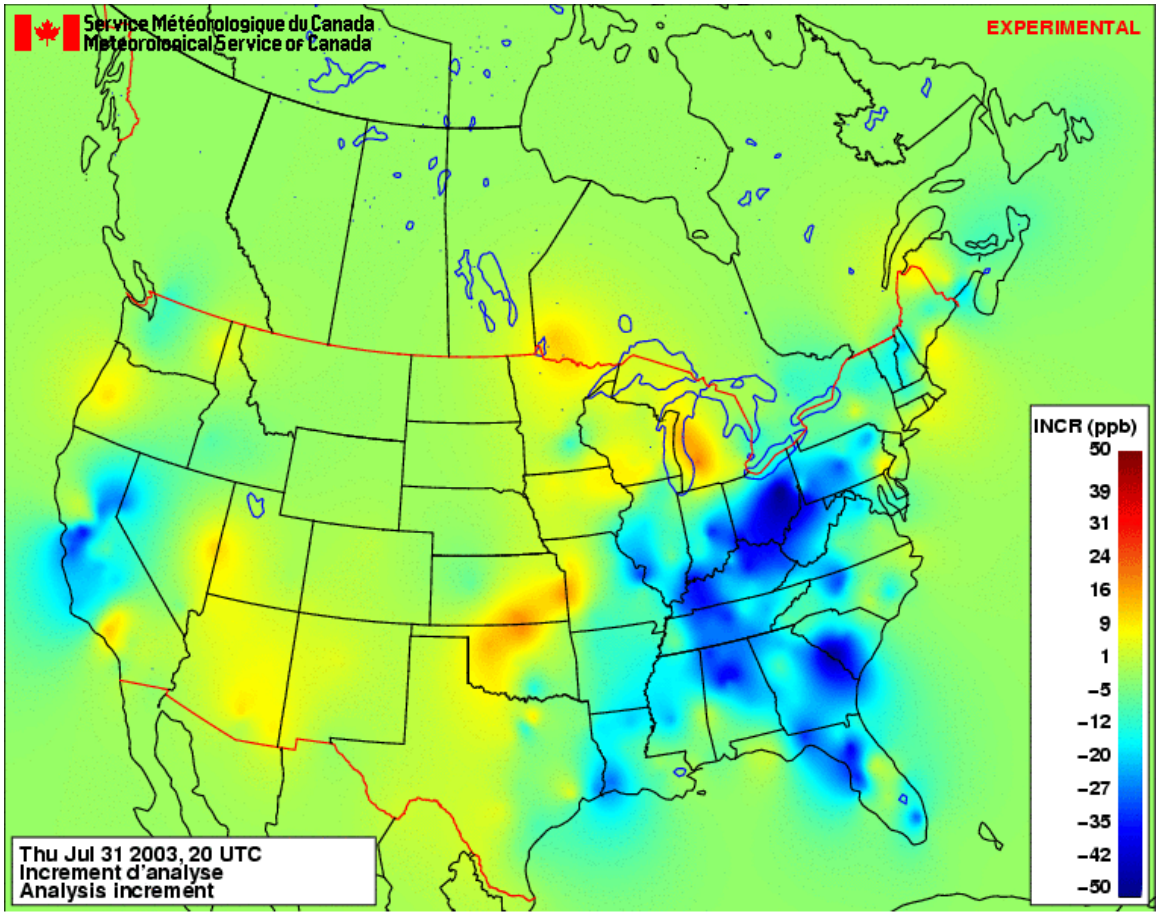

FIGURE 11C. Analysis increment for July 31 2003 at 20Z.

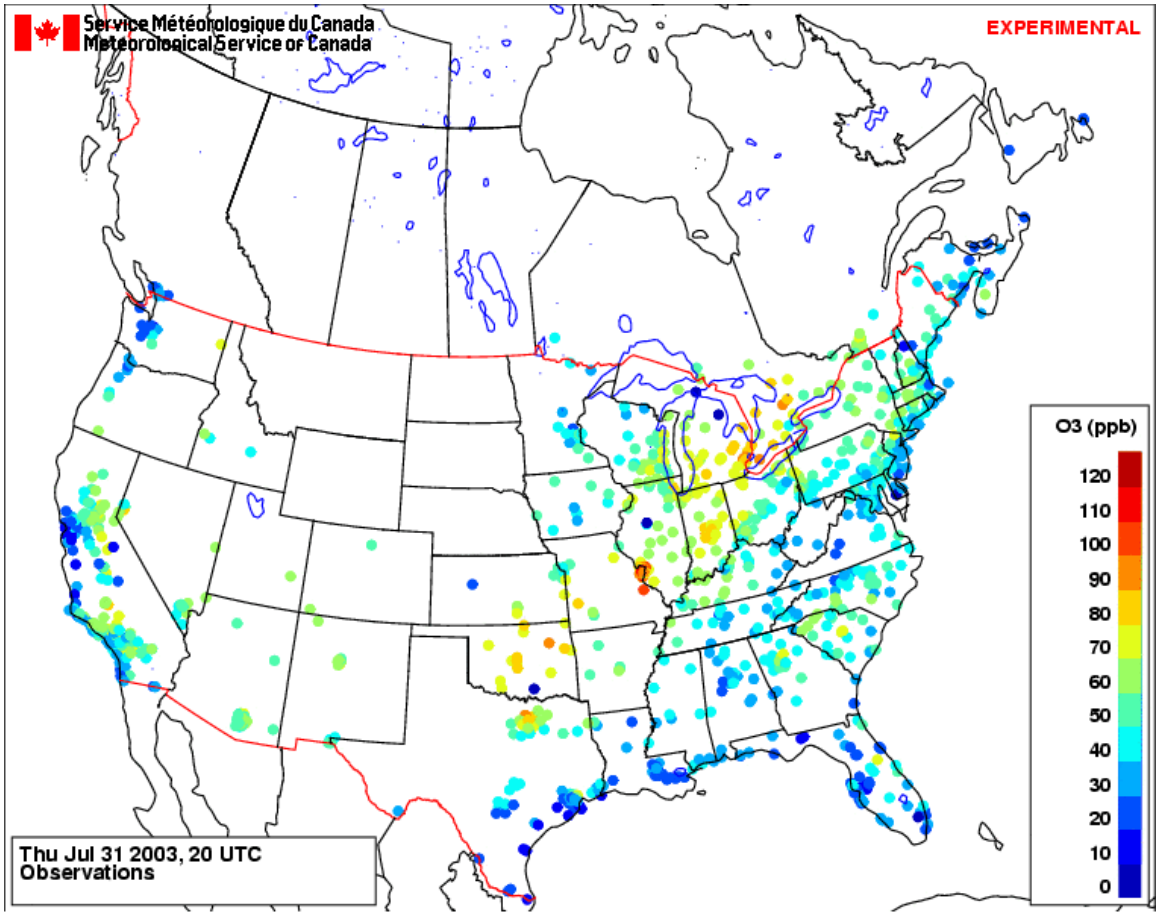

FIGURE 11D. Observations for July 31 2003 at 20Z.

For the case of July 31 2003 at 20Z, we find again that CHRONOS model significantly overpredicts and over roughly the same regions. A regular inspection of analysis increment during July and August 2003 have revealed consistent pattern of negative analysis increment in Eastern US and Southern California and positive increment along the Northwest Coast of North America. Those patterns give insights into model behavior. For example, persistant negative analysis increments (overprediction) over regions of high anthropogenic emissions density (see figure 9) is consistant with the fact of likely inadequate fields of prescribed emissions. On the other hand, persistant positive increments over the Northwest US and West Coast of Canada suggests that stratospheric ozone which usually replenishes the background noise (phenomenon missing in CHRONOS model) affects those regions more likely because of lack of pollution sources upstream. Finally, during cold fronts episodes or other well organized weather systems, analysis increments were found to match clouds indicating a potential problem with the cloud fraction seen by CHRONOS model[9].

Scatter plot of model against observations and objective analysis against observations are given in figure 12. Results again show dramatic improvement of the correlation coefficient

[9] This bug is being corrected in CHRONOS at the time of writing this report by lifting model top to include more upper levels.

(r^2 increases from 0.35 for X_b in figure 12A to 0.69 for X_a in figure 12B) with a reduction of a factor about 2 of the RMSE for the regression fit. The mean bias drops from -8.4 to -1.

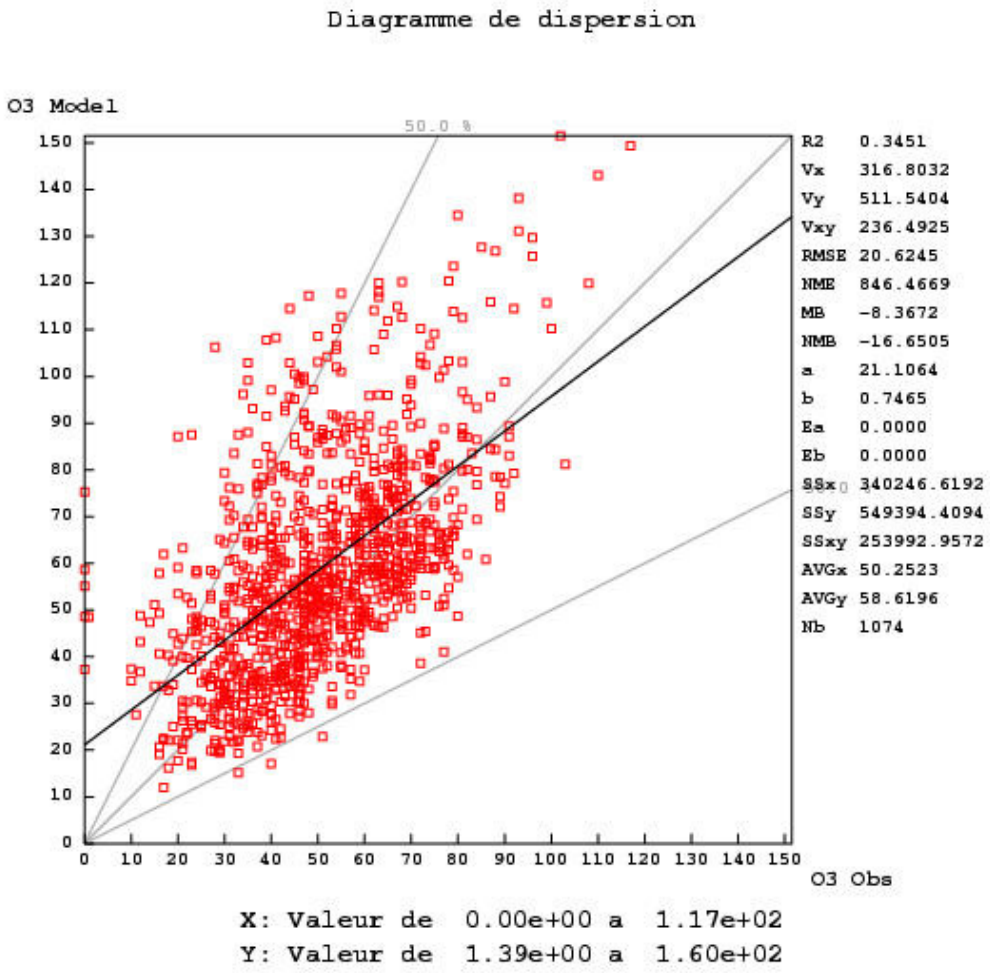

FIGURE 12A. Scatter plot and regression fit for X_b against observations for July 31 2003 at 20Z.

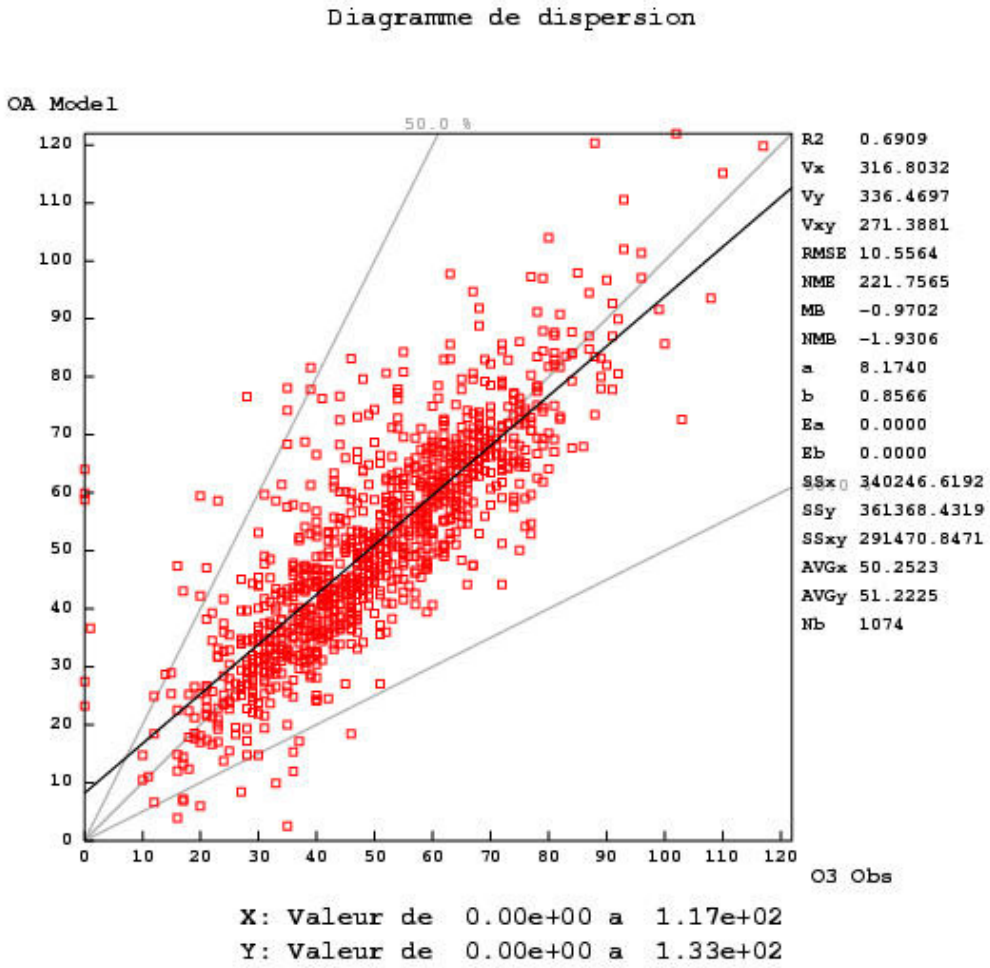

FIGURE 12.B. Scatter plot and regression fit for X_a against observations for July 31 2003 at 20Z.

c) case study of August 30 2002 at 00Z

For cases during August 2002, correlation coefficient are even higher as compared for those cases in July 2003 shown above. As an example, the explained variance (given by r^2) of OA vs observations is about 0.88 (figure 13B) as compared with 0.69 for the CHRONOS output (figure 13A) for August 30 2002 at 00Z. The relatively high correlation of the model (figure 13A) could be explained with better performance of CHRONOS during pollution episodes and for certain hour of the day (such as 00Z). As far as OA is concerned, (figure 13B) an additional explanation for the even higher correlation is the fact that error statistics were originally calculated for the period of August 2002. Since this case falls during the same period which was used to build model error statistics, it is not surprising to obtain such high values for the coefficient of correlation (Xa versus

observations in figure 13b). This illustrates the variability of error statistics from one year to another as far as summer is concerned and explains why the XHI square test sometimes shows values far from the expected value of 1 (for OA using unbiased innovation).

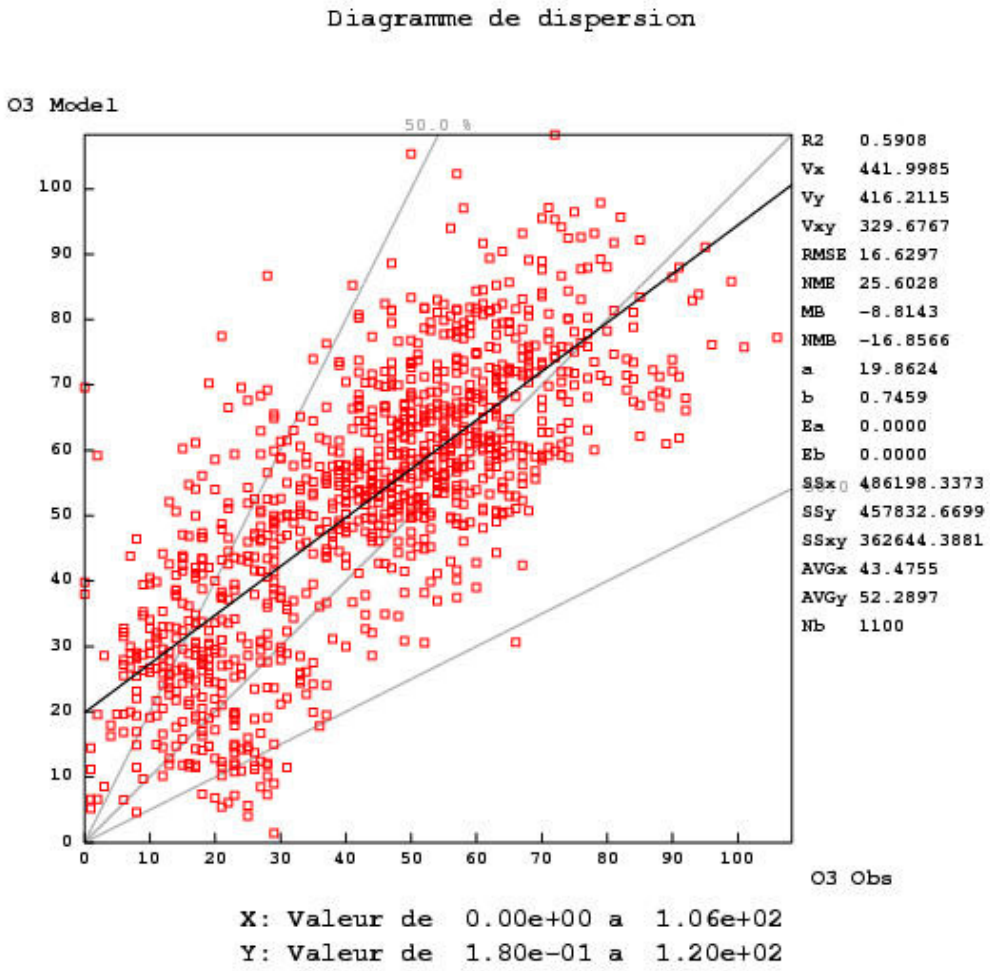

Figure 13A. Scatter plot Chronos output vs observations for August 30 2002 at 00Z.

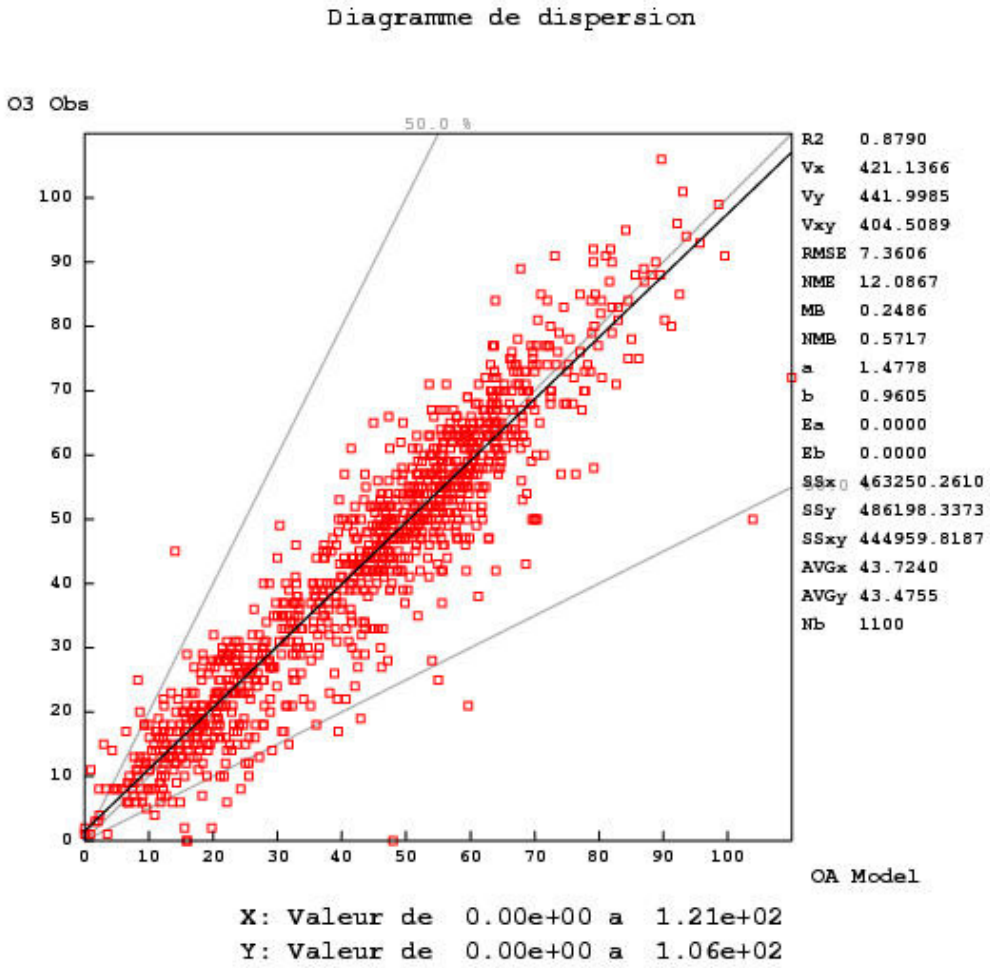

Figure 13B. Scatter plot OA output vs observations for August 30 2002 at 00Z.

7) ALGORITHM AND COMPUTER PROGRAMS IN OPERATIONAL CONFIGURATION

Since July 4th 2003 at 6Z, the objective analysis and incremental analysis fields for surface ozone has been available on the internal MSC Web Page as an experimental product (http://iweb.cmc.ec.gc.ca/~afsgmof/CTM/CTMframe.html).
The computer scripts for data transfer were written in Unix and TCL and the program which calculates analysis increment in Fortran 90. Annex 1 gives the algorithm and logic for the Version 1.0 of Objective Analysis for surface ozone. Annex 2 provides the code for each blocks described below.

Here is the basic flow of main steps involved in producing the OA map in the operational configuration and the complete path of the appropriate code:

1) **cronfile**: clock triggers the launching of OA driver at appropriate time (usually 0:45 past the hour)
/users/dor/afsr/air/crontab/pollux
2) **driver is launched**: starts the Objective analysis cycle
/users/dor/afsr/air/cron/script/analyseobjective
3) get observations from EPA site
/users/dor/afsr/air/cron/script/GetEPA
4) brings all data together and calculates innovation
/users/dor/afsr/air/cron/script/OA_getInput.tcl
5) calculate analysis increment
/users/dor/afsr/air/cron/src/increment/increment.f90
6) output analysis increment and produce OA map
/users/dor/afsr/air/cron/script/OA_obsGrid.tcl

Archives of all the output products including the Chi-square diagnosis and a file containing real-time innovation are to be found (for the current month) at the following path:
/users/dor/afsr/air/cron/data/analyseobejctive.
The file**: archiveOA_YYYY/MM.txt** contains the fields X_a,X_b and analysis increment whereas **xhicar-YYYYMM.txt** contains archives for the Chi-square diagnosis.
Note that observations in real-time are stored in:
/users/dor/afsr/air/cron/data/Obs/O3.

At the end of the month, local archives are transferred to a long term archive system on tape (CFS): **/users/dor/afsr/air/archives_OA.**

8) VERIFICATION OF OBJECTIVE ANALYSIS

Verification were performed at two levels; 1) in the developmental phase where rigorous and extensive tests were used (off-line) and 2) in the operational configuration (on-line) where two diagnostic tools are utilized: a) Chi-square diagnostic and 2) comparison of the scatter plot OA vs observation with the scatter plot of model vs observation.

- DEVELOPMENTAL MODE (off-line)

In order to demonstrate the feasibility of OA for surface ozone, extensive verification must be done before implementation. Several checks were performed in this phase: check if 1) eigenvalues of the matrix A were all positive (see section on THEORY), 2) the variance of O-A (variance of innovation of objective analysis is reduced compared to the variance of O-P (variance of innovation of model). The latter test has to be done by using an independent set of stations to verify (about 1/3 of stations used for verification and 2/3 used for producing the OA field) and is shown below.

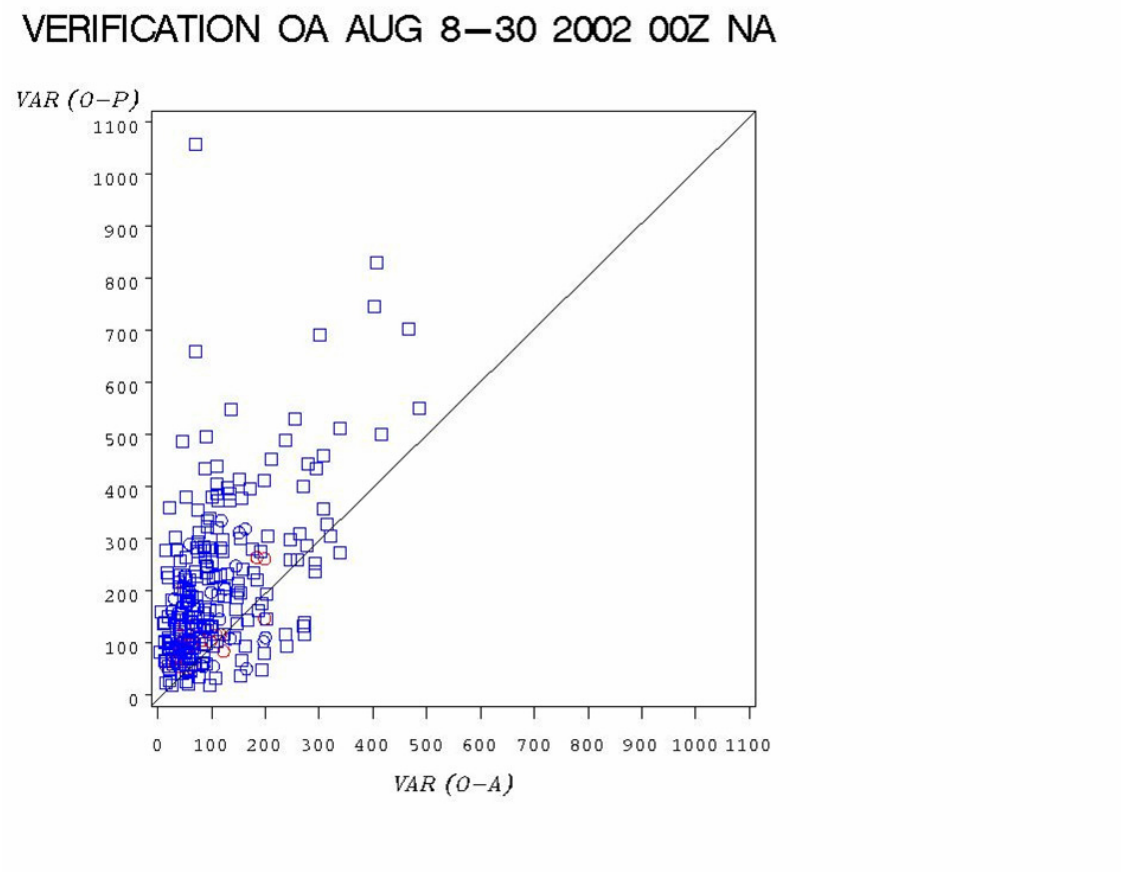

Figure 14A.

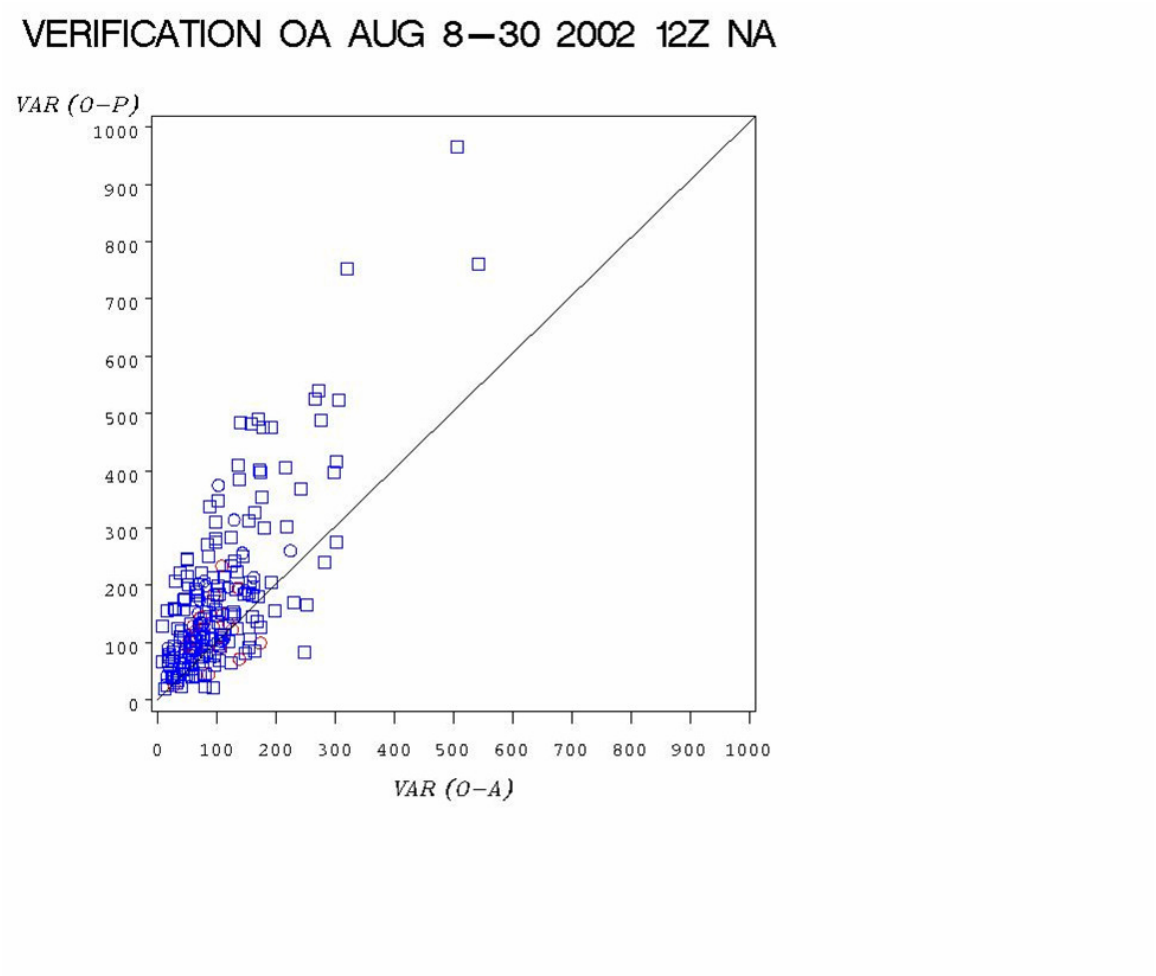

Figure 14 B.

Figure14 shows the error variance of observation minus prediction (var O-P) plotted against the error variance of model against observation (var O-A) for A) 00Z and B) 12Z. Note that circles indicate stations selected for verification for more than 50% of the days whereas squares indicate stations selected between 25-50% of the days for verification. Red color indicates Canadian stations and blue, US stations.

For verification purposes, the selection of stations were randomly done for each individual day of the study period. This is to avoid any possible bias in the process of selection. Figure 14 show that stations lying to the left of the 1:1 straight line have reduced their variance of error with OA (var(O-A)) as compared with that of model (var(O-P)). This reduction of variance with OA happens for the majority of stations as it should do. Most of stations have reduced the variance of errors by a factor of 2 or more.

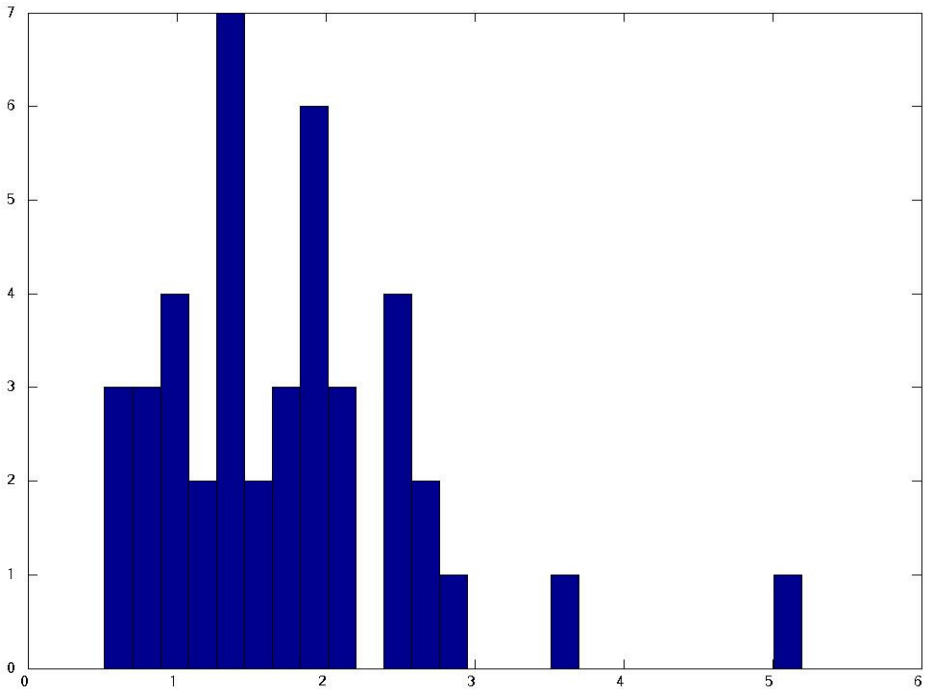

ratio var(O-P)/var(O-A)

FIGURE 15A. Distribution frequency of number of stations against ratio var(O-P) divided by var(O-A). The data set used is from Aug 8-30 2002 at 12Z.

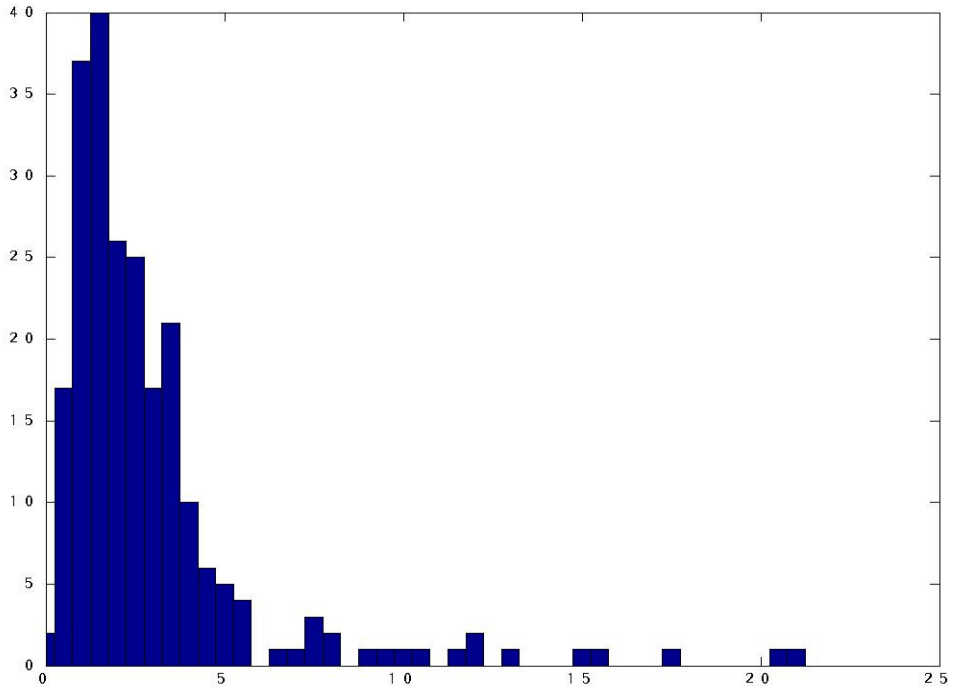

ratio var(O-P)/var(O-A)

FIGURE 15B. Distribution frequency for number of stations against ratio var(O-P) divided by var(O-A). The data set used is from Aug 8-30 2002 at 00Z.

Figure 15A and B show histograms of the ratio of var(O-P)/var(O-A**).** A ratio less than 1 indicates a deterioration introduced by OA whereas a ratio over 1 indicates an improvement of the error variance caused by OA. In Figure 15A, for about 36 stations, the ratio is about equal or superior to 1 whereas for only 6 stations it is below 1 (between 0.5 and 1). In Figure 15B, most stations also show a ratio over 1 although we note the fact that we can observe a little bit more deterioration (number of stations having their ratio less than 1) at 00Z when compared to the case of 12Z. This could be explained by the fact that model error and bias is larger at 00Z than at 12Z (see figure 6). Nevertheless, in both figures, a big majority of stations have reduced their error variance with OA as it should be.

At 12 and 00Z , most stations reduce their error variance by about a factor 2. At 00Z, at least one station has a reduction factor of 21. This clearly shows the potential power of improving accuracy with field X_a (objective analysis).

- OPERATIONAL MODE (on line)

In the operational mode it is desirable to use the maximum number of stations to produce the OA field. Therefore, no independent set of stations is used for the sole purpose of verification in this configuration. Therefore, scatter plots var(O-P) versus var(O-A) are not presented here. However, verification was done using the Chi-square statistics. Such

verification was done for August 2002. Along with Chi-square values, the coefficient of correlation for model and objective analysis fields unbiased (BIAS=0) and biased (BIAS not equals 0) against observations are shown below.

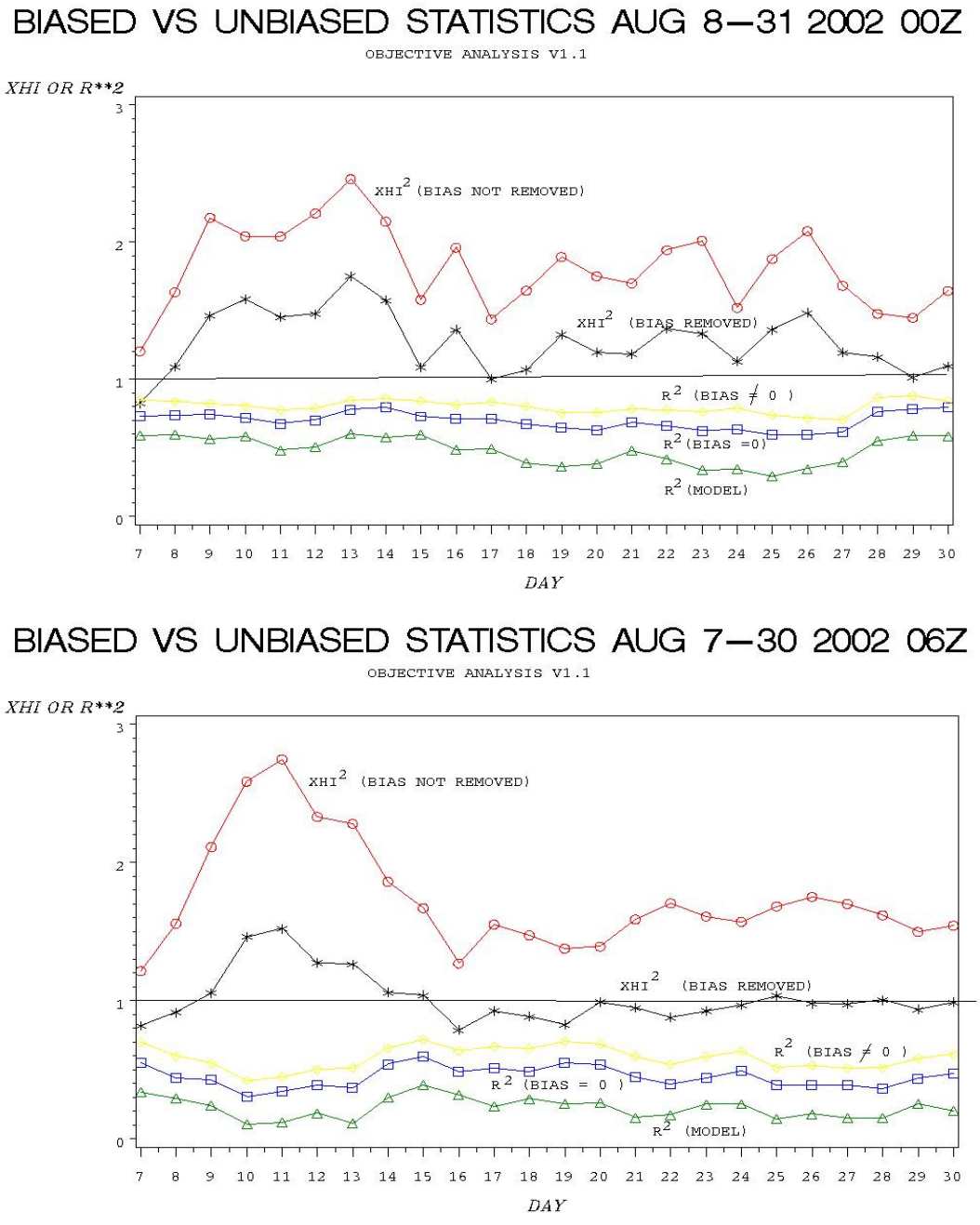

FIGURE 16. Verification for 00Z (A) and 06Z (B).

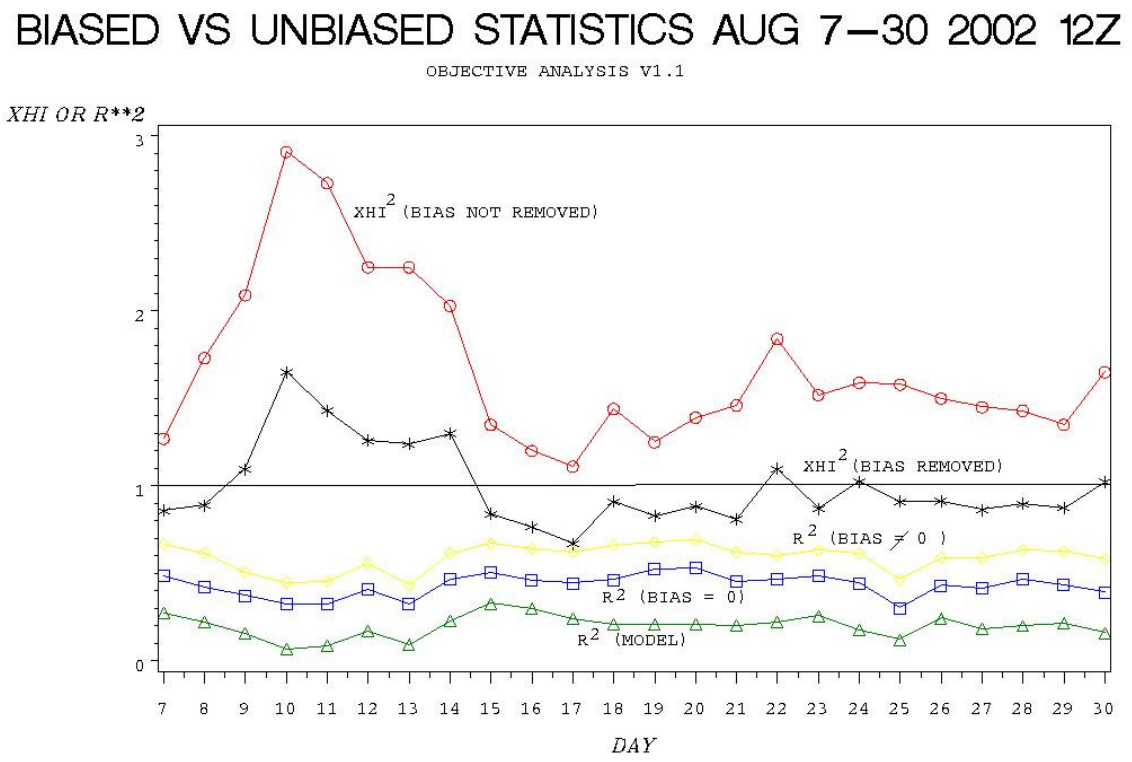

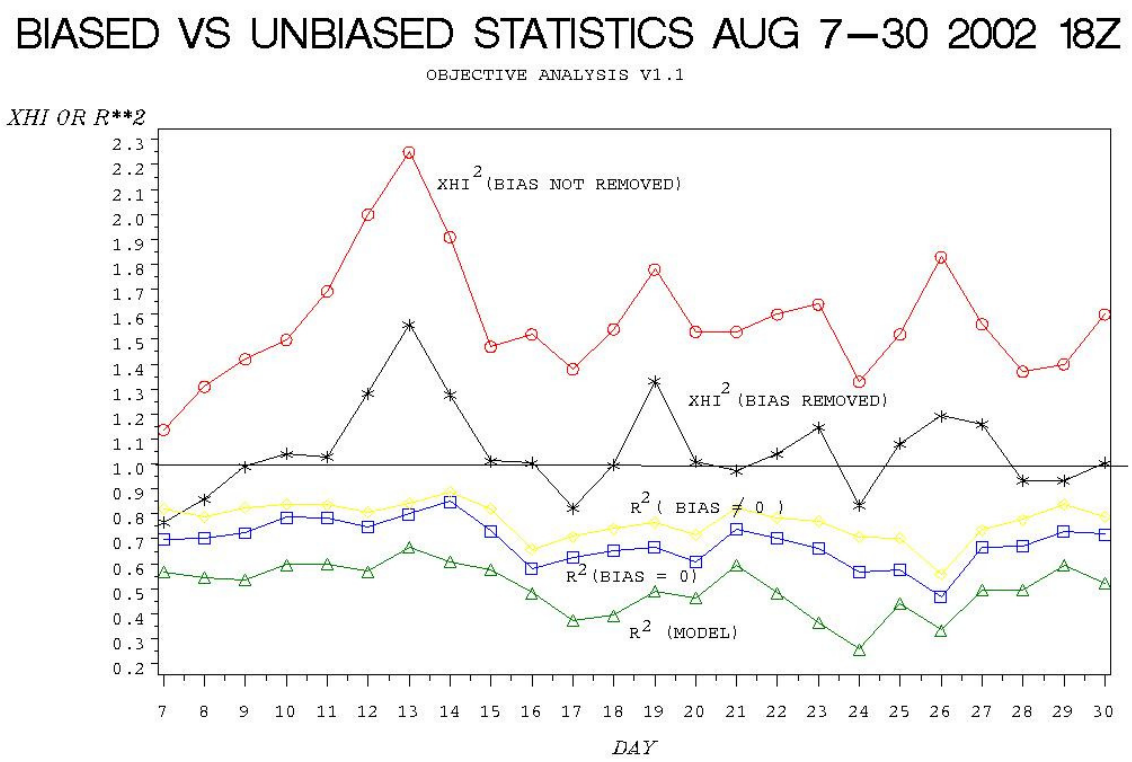

FIGURE 16 (contd). Verification of OA for 12Z (C) and 18Z (D).

Figure 16A,B,C and D show the XHI squared statistics for the case of unbiased innovation (bias removed or BIAS =0) and bias not removed (B not equals 0) for four times of the day (00Z,06Z,12Z and 18Z) for the period August 7 – 30 2002. As it should be, the XHI squared value average around 1 when the bias of innovation is removed for all periods. At the bottom part of each figures are plotted r squared (variance explained or squared coefficient of correlation) of OA vs observations for each day of the period at a given hour. Results show that 1) R squared is significantly higher for OA (bias removed or not) than for the CHRONOS output (labeled as R^2 (Model)), 2) the best results for the coefficient of correlation are found when the bias is not removed even if the XHI squared statistics does no longer average to one. For this reason, it was decided not to remove the bias for the operational version of OA.

SUMMARY AND CONCLUSIONS

On July 4th 2003, for the first time at CMC (Canadian Meteorological Center) and within the MSC (Meteorological Service of Canada), an objective analysis map for **surface ozone** was produced on an experimental basis in the context of a " semi-operational configuration ". The theory of OI (optimal interpolation) with no data selection has been used to build up the OA system so that it makes it equivalent to a 2D-VAR analysis. In this study, CHRONOS model outputs (V2.3.6) for surface ozone are combined with EPA-AIRNOW ozone real-time data base (over 1400 reporting stations).

Verification of objective analysis versus observations in both R&D and operational mode have demonstrated relatively good results so far. Moreover, a regular inspection of analysis increment during August 2002, July and August 2003 have revealed consistent patterns of negative analysis increments in Eastern US and California and positive increment along the Northwest Coast of North America. Those patterns give deep insights into model behavior. On the other hand, representativeness of some stations which displays very local signal is an issue which remain to be addressed and is considered as a research topic.

It was found that FOAR modeling (First Order Autoregressive Model) is more suitable to estimate model error statistics for surface ozone than SOAR (Second Order Autoregressive model) or TOAR (Third Order Autoregressive model) fittings usually adopted in meteorology for Objective analysis or data assimilation.

The usefulness of OA maps is wide: 1) initialization of air quality models 2) provide the users with a more spatially complete and accurate analysis surface ozone (as compared with model output or observations alone) 3) bring deep insights into possible model erroneous behavior or bugs. Finally, it is suggested that those maps of OA can be used to construct a sound ozone climatology, seasonal maps of SUM60, AOT40 or other specialized index which links the impact of air pollution and environmental impacts.

The work done in the context of this report is the first building block towards a full system of data assimilation for surface chemical species.

ACKNOWLEDGMENTS

The authors wish to thank Stéphane Gaudreault and Jean-Philippe Gauthier for their valuable contribution and assistance in the implementation phase of the operational version of OA.

REFERENCES

- **Bouttier F., Courtier P**., 2000. ECMWF Lecture Notes on Data Assimilation (available from ECMWF Web site).
- **Daley R**., 1991. Atmospheric data analysis. Cambridge University Press, Atmospheric ands Space Science Series, 457 pages.
- **Daley R.,** 1992. « The lagged innovation covariance : a performance diagnostic for atmospheric data assimilation. ». Monthly Weather Review 120., pp. 178-196.
- **Gauthier P., Charrette C., Fillion L., Koclas P., Laroche S.**, 1999. « Implementation of a 3D Variational data assimilation system at the Canadian Meteorological Centre . Part I: The Global Analysis. Atmosphere Ocean, vol. XXXVII, No. 2., pp. 103-156., June 1999.
- **Hollingsworth A. and P. Lonnberg**, 1986. " The statistical structure of short-range forecast errors as determined from radiosonde data ". Part I: the wind field. Tellus, 38A: 111-136.
- **Ménard R., Chang L.P., Larson J.W**., 1999. "Application of a robust chi-square validation diagnostic in PSAS and Kalman filtering experiments", in Proceedings of the Third International Symposium on Asssimilation of Observations in Meteorology and Oceanography, Quebec City, 7-11 June 1999. WWRP Report series, no 2.. Technical Document, WMO/TD – No. 986.
- **Ménard R**., 2000. "Tracer assimilation" in Inverse Methods in Global Biogeochemical Cycles". Geophysical Monograph 114. AGU.
- **Mitchell H, C. Chouinard C., Charette C., Hogue R., Lambert S.J**., 1996. "Impact of a revised analysis algorithm on an operational data assimilation". Monthly Weather Review., 124, pp. 1243-1255.
-**Pudykiewicz J., A. Kallaur, and P.K. Smolarkiewicz**, 1997. "Semi-Lagrangian modeling of tropospheric ozone. Tellus, 49B, 231-248.
- **Robichaud A., Kallaur A., Pudykiewicsz J., Menard R., Moffet R**.: " Impacts of a new gas dry deposition module on Chronos model error". Oral presentation at CMOS Congress, Ottawa, June 2-5 2003.
- **Rutherford I., 1972.** "Data assimilation by statistical interpolation of forecast error fields". J.Atmos.Sci., 29, pp. 809-815.
- **Tilmes S**., "Verfahren zur Analyse von Messungen atmospharischer Spurengase mit dem Ziel der Assimilation in Chemie-Transportmodellen", Berichte des Deutschen Wetterdienstes, no. 207., 1999.
- **Zhang L., Brook J.R., Vet R., 2002**. " On ozone dry deposition – with emphasis on non-stomatal uptake and wet canopies. Atmos. Env., 36 (2002), 4787-4799.

ANNEX 1. Algorithm of an operational OA system

ANNEX 2. Computer code used in the operational version V1.01.